

# Optimized Baxter Model of Protein Solutions: Electrostatics versus Adhesion

Peter Prinsen and Theo Odijk\*,

*Complex Fluids Theory, Faculty of Applied Sciences,  
Delft University of Technology, Delft, the Netherlands*

## Abstract

A theory is set up of spherical proteins interacting by screened electrostatics and constant adhesion, in which the effective adhesion parameter is optimized by a variational principle for the free energy. An analytical approach to the second virial coefficient is first outlined by balancing the repulsive electrostatics against part of the bare adhesion. A theory similar in spirit is developed at nonzero concentrations by assuming an appropriate Baxter model as the reference state. The first-order term in a functional expansion of the free energy is set equal to zero which determines the effective adhesion as a function of salt and protein concentrations. The resulting theory is shown to have fairly good predictive power for the ionic-strength dependence of both the second virial coefficient and the osmotic pressure or compressibility of lysozyme up to about 0.2 volume fraction.

Address for correspondence: T. Odijk, P.O. Box 11036 2301 EA Leiden, the Netherlands

## I. INTRODUCTION

It has been intimated that the solution properties of globular proteins may bear relation with their crystallization properties [1, 2]. Since the characterization of proteins commands ever more attention, such a contention is of considerable interest so much work has been carried out on this topic recently [3, 4, 5, 6, 7, 8].

The difficulty of setting up a predictive theory of protein suspensions based on what is known about the interaction between two proteins, has been acknowledged for some time [9]. Best fitting of the osmotic pressure of, for instance, bovine serum albumin up to 100 g/l, leads to effective excluded volumes whose behavior as a function of salt is enigmatic [10].

In recent years, there has been a tendency to forget about all detail of the protein interaction altogether—both attractive and repulsive—and simply introduce a single adhesion parameter [10, 11, 12, 13, 14]. Despite the electrostatic repulsion which is substantial, the data are often merely rationalized in terms of the bare protein diameter within the context of an adhesive sphere model and such an approach seems to have merit [10, 11, 12, 13, 14]. This empiricism has prompted us to develop a theory of screened charged protein spheres that have a constant stickiness, where the electrostatic interaction is compensated, in part, by the adhesive forces. Thus, we argue that, effectively, the spheres are assigned a hard diameter identical to the actual diameter provided the remnant adhesive interaction now depends on the electrolyte and protein concentrations in a manner to be determined variationally. First, we analyze the second virial coefficient as such, for this will point toward a way of dealing with the osmotic pressure at nonzero concentrations. We focus on experiments with lysozyme, a protein which is reasonably spherical and has been well studied for a long time [15].

## II. SECOND VIRIAL COEFFICIENT

### A. Theory

#### 1. *Second virial coefficient*

The second virial coefficient  $B_2$  describes the first order correction to Van 't Hoff's law

$$\frac{\Pi}{\rho k_B T} = 1 + B_2 \rho + O(\rho^2). \quad (1)$$

Here,  $\Pi$  is the osmotic pressure of the solution,  $\rho$  is the particle number density,  $k_B$  is Boltzmann's constant and  $T$  is the temperature. From statistical mechanics we know that, given the potential of mean force  $U(\mathbf{r})$  between two spherical particles whose centers of mass are separated by the vector  $\mathbf{r}$ , one can calculate  $B_2$  from

$$B_2 = -\frac{1}{2} \int_V d\mathbf{r} f(\mathbf{r}) \quad (2)$$

where  $f(\mathbf{r}) = e^{-U(\mathbf{r})/k_B T} - 1$  is the Mayer function. In principle, the interaction  $U(\mathbf{r})$  may be determined from experimental data on the second virial coefficient by suitable Laplace inversion. This has been done for atoms and spherically symmetric molecules [16, 17], for which the second virial coefficient has been measured over a broad enough range of temperatures. One might think of formulating a procedure similar in spirit and applicable to protein solutions, but with the ionic strength as independent variable instead of the temperature. However, to be able to determine an accurate approximation of the interaction, the experimental data have to be known fairly accurately, which is not the case at hand, as will become clear further on. We are therefore forced to adduce presumptions about the interaction.

We assume the protein to be spherical with radius  $a$ , its charge being distributed uniformly on its surface. For convenience, all distances will be scaled by the radius  $a$  of the sphere and all energies will be in units of  $k_B T$ . Because monovalent ions (counterions and salt ions) are also present in solution, there will be a screened Coulomb repulsion between the proteins, here given by a far-field Debye-Hückel potential. We compute the effective charge  $qZ_{eff}$  in the Poisson-Boltzmann approximation where  $q$  is the elementary charge. For now, we let the attraction between two proteins be of short range, and we model it by a potential well

of depth  $U_A$  and width  $\delta \ll 1$ . The total interaction  $U(x)$  between two proteins is of the form

$$U(x) = \begin{cases} \infty & 0 \leq x < 2 \\ U_{DH}(x) - U_A & 2 \leq x < 2 + \delta \\ U_{DH}(x) & x \geq 2 + \delta \end{cases}, \quad (3)$$

$$x \equiv \frac{r}{a},$$

with Debye-Hückel potential [18]

$$U_{DH}(x) = 2\xi \frac{e^{-\mu(x-2)}}{x}. \quad (4)$$

Here,  $\xi \equiv \frac{Q}{2a} \left( \frac{Z_{eff}}{1+\mu} \right)^2$ ,  $\kappa^{-1}$  is the Debye length defined by  $\kappa^2 = 8\pi QI$ ,  $I$  is the ionic strength,  $Q = q^2/\epsilon k_B T$  is the Bjerrum length, which equals 0.71 nm in water at 298 K,  $\epsilon$  is the permittivity of water and  $\mu \equiv \kappa a = 3.28a\sqrt{I}$  in water, if  $a$  is given in nm and  $I$  in mol/l. We suppose 1-1 electrolyte has been added in excess so  $I$  is the salt concentration.

In order to evaluate  $B_2$  analytically, we have found it expedient to split up  $B_2$  into several terms:

$$B_2 = B_2^{HS} \left( 1 + \frac{3}{8}J \right), \quad (5)$$

where  $B_2^{HS} = 16\pi a^3/3$  is the second virial coefficient if the proteins were merely hard spheres and we introduce integrals

$$J \equiv \int_2^\infty dx x^2 (1 - e^{-U(x)}) \equiv J_1 - (e^{U_A} - 1) J_2, \quad (6)$$

$$J_1 \equiv \int_2^\infty dx x^2 (1 - e^{-U_{DH}(x)}), \quad (7)$$

$$J_2 \equiv \int_2^{2+\delta} dx x^2 e^{-U_{DH}(x)}. \quad (8)$$

Here,  $J_1$  is the value of  $J$  in the absence of attraction and may be simplified by Taylor expanding the Boltzmann factor in the integrand for small values of  $U_{DH}$  to second order. However, to increase the accuracy of the expansion, we adjust the coefficient of the second order term so that the approximation to the integrand coincides with its actual value at  $x =$

2, i.e., we approximate  $x(1 - e^{-U_{DH}(x)}) \simeq 2\xi e^{-\mu(x-2)} - 2\alpha\xi^2 e^{-2\mu(x-2)}$ , with  $\alpha = \frac{e^{-\xi}(1-\xi)}{\xi^2}$ , resulting in

$$J_1 \simeq \frac{4(\mu + \frac{1}{2})\xi}{\mu^2} \left(1 - \frac{\alpha}{2}\xi\right), \quad (9)$$

where we have neglected the small term  $\alpha\xi^2/2\mu^2$ . For instance, in the case of lysozyme, the deviation of the approximation Eq. (9) from the exact result is smaller than about 3% for  $I \geq 0.05$  M and smaller than about 1% for  $I \geq 0.2$  M. Since  $\delta \ll 1$ ,  $J_2$  may be simplified by using the trigonometrical approximation  $\int_2^{2+\delta} dx g(x) \simeq \frac{1}{2}\delta [g(2) + g(2 + \delta)]$ , which leads to

$$J_2 \simeq 2\delta \left[ e^{-\xi} + \left(1 + \frac{\delta}{2}\right)^2 e^{-\frac{\xi}{1+\delta/2}e^{-\mu\delta}} \right]. \quad (10)$$

It is important to note that  $\mu\delta$  may be greater than unity even if  $\delta \ll 1$ . Again, for lysozyme, this approximation deviates less than about 3% from the exact value for  $I \geq 0.2$  M and  $\delta \leq 0.5$  and less than about 1% for  $I \geq 0.2$  M and  $\delta \leq 0.15$ .

## 2. *Effective attractive well*

We next present a discussion of  $B_2$  in terms of equivalent interactions and their Mayer functions even though the analysis of the previous section is self-contained. Sections IIA2 and IIA3 may be viewed as preludes to the formulation of the liquid-state theory developed in section III. At large separations ( $x > 2 + \delta$ ), the interaction between the particles is purely repulsive, leading to a positive contribution to the second virial coefficient. If, at a certain ionic strength, the second virial coefficient is smaller than the hard-core value ( $B_2 < B_2^{HS}$ ), this positive contribution is necessarily cancelled by only part of the negative contribution of the attractive interaction at small separations, the part, say, between  $x = 2 + \epsilon_0$  and  $x = 2 + \delta$ , see Fig. 1. The remaining potential which we will call an effective attractive well, then consists of a hard-core repulsion plus a short-range attraction of range  $\epsilon_0$ . The value of  $\epsilon_0$  is determined by noting that the free energy of the suspension must remain invariant, which, in the asymptotic limit of low densities, leads to the identity

$$B_{2,\epsilon_0} = B_2, \quad (11)$$

where  $B_2$  is the second virial coefficient of the previous section and  $B_{2,\epsilon_0}$  is the second virial coefficient pertaining to the effective attractive well. Using Eq. (2), we rewrite Eq. (11) as

$$\int_V d^3\mathbf{r} \Delta f = 0, \quad (12)$$

in terms of the difference in the respective Mayer functions

$$\Delta f \equiv f - f_{\epsilon_0}, \quad (13)$$

where  $f$  is the Mayer function of the original interaction and  $f_{\epsilon_0}$  is the Mayer function of the effective attractive well. In dimensionless units, Eq. (12) is equivalent to the condition

$$\int_{2+\delta}^{\infty} dx x^2 (1 - e^{-U_{DH}(x)}) = \int_{2+\epsilon_0}^{2+\delta} dx x^2 (e^{U_A} e^{-U_{DH}(x)} - 1), \quad (14)$$

where, using the same approximation that led to Eq. (9), we write

$$\int_{2+\delta}^{\infty} dx x^2 (1 - e^{-U_{DH}(x)}) \simeq \frac{2\xi e^{-\mu\delta}}{\mu} \left(1 - \frac{\alpha}{2}\xi e^{-\mu\delta}\right) \left(2 + \delta + \frac{1}{\mu}\right) \quad (15)$$

and, using  $\int_{2+\epsilon_0}^{2+\delta} dx x^2 \Delta f(x) \simeq 2(\delta - \epsilon_0) [\Delta f(2 + \delta) + \Delta f(2 + \epsilon_0)]$ ,

$$\int_{2+\epsilon_0}^{2+\delta} dx x^2 (e^{U_A} e^{-U_{DH}(x)} - 1) \simeq 2(\delta - \epsilon_0) \left[-2 + e^{U_A} \left(e^{-\frac{\xi}{1+\delta/2} e^{-\mu\delta}} + e^{-\frac{\xi}{1+\epsilon_0/2} e^{-\mu\epsilon_0}}\right)\right]. \quad (16)$$

To leading order, we then find an explicit relation for  $\epsilon_0$

$$\delta - \epsilon_0 \simeq \frac{\xi e^{-\mu\delta}}{\mu e^{U_A}} e^{\xi e^{-\mu\delta}}, \quad (17)$$

which works well at high ionic strengths (i.e. at low values of  $\xi$ ), e.g. whenever  $I \geq 1$  M in the case of lysozyme at pH 4.5. A more accurate value of  $\delta - \epsilon_0$  is obtained by equating Eqs. (15) and (16), and then iteratively updating the factor  $(\delta - \epsilon_0)$ , starting with the initial value  $\epsilon_0 = \delta$ .

The second virial coefficient pertaining to the original potential  $U(x)$  (Eq. (3)) is now rewritten as

$$B_2 = B_{2,\epsilon_0} = B_2^{HS} \left(1 + \frac{3}{8} \int_2^{2+\epsilon_0} dx x^2 (1 - e^{U_A} e^{-U_{DH}(x)})\right). \quad (18)$$

The depth  $U_A - U_{DH}(x)$  does not vary strongly though, since  $\epsilon_0 \ll 1$ , so, to simplify things computationally, let us approximate the interaction by a square well potential,

$$U_{SW}(x) = \begin{cases} \infty & 0 \leq x < 2 \\ -U_S & 2 \leq x < 2 + \epsilon_0 \\ 0 & x \geq 2 + \epsilon_0 \end{cases}. \quad (19)$$

We choose  $U_S$  in such a way that  $B_2 = B_2^{SW}$  or, equivalently,

$$\int_2^{2+\epsilon_0} dx x^2 (e^{U_S} - e^{U_A} e^{-U_{DH}(x)}) = 0. \quad (20)$$

To leading order in  $\epsilon_0$ , we have

$$\int_2^{2+\epsilon_0} dx x^2 e^{U_S} \simeq 4\epsilon_0 e^{U_S}, \quad (21)$$

and, using the approximation  $\int_2^{2+\epsilon_0} dx x^2 g(x) \simeq 2\epsilon_0 [g(2 + \epsilon_0) + g(2)]$ , we write

$$\int_2^{2+\epsilon_0} dx x^2 e^{U_A} e^{-U_{DH}(x)} \simeq 2\epsilon_0 e^{U_A} \left[ e^{-\xi} + e^{-\frac{\xi}{1+\epsilon_0/2}} e^{-\mu\epsilon_0} \right]. \quad (22)$$

The depth  $U_S$  of the potential is then given by

$$e^{U_S} \simeq \frac{1}{2} e^{U_A} \left( e^{-\xi} + e^{-\frac{\xi}{1+\epsilon_0/2}} e^{-\mu\epsilon_0} \right) \quad (23)$$

in terms of the original variables. Finally, we point out that the two attractive wells that we have introduced are physically meaningful only if  $B_2 < B_2^{HS}$ .

### 3. Attractive well in the Baxter limit

We have shown that one may simplify the statistical thermodynamics of the protein suspension at low densities considerably, by replacing the original interaction, consisting of an electrostatic repulsion and a short-range attraction, by a single attractive well of short range. The electrostatic interaction may be substantial but it is compensated by part of the original attractive well which is quite strong ( $U_A > 1$ ). Another useful interaction expressing attractive forces of short range consists of a hard-sphere repulsion and an attraction of infinite strength and zero range, namely the adhesive hard sphere (AHS) potential of Baxter [19]

$$U_{AHS}(x) = \begin{cases} \infty & 0 \leq x < 2 \\ \log \frac{12\tau\omega}{2+\omega} & 2 \leq x \leq 2 + \omega \\ 0 & x > 2 + \omega \end{cases}, \quad (24)$$

where  $\tau$  is a constant and the limit  $\omega \downarrow 0$  has to be taken after formal integrations. The second virial coefficient remains finite

$$B_2^{AHS} = B_2^{HS} \left( 1 - \frac{1}{4\tau} \right). \quad (25)$$

Because much is known about the statistical mechanics of the Baxter model, one often defines  $\tau$  in terms of some  $B_2$  and naively assumes there is a one-to-one correspondence between the

original and Baxter models. For instance, in our case,  $B_2^{AHS} = B_2 = B_{2,\epsilon_0} = B_2^{SW}$ . Since we have

$$\begin{aligned} B_2^{SW} &= B_2^{HS} \left( 1 - (e^{U_S} - 1) \left[ \left( 1 + \frac{\epsilon_0}{2} \right)^3 - 1 \right] \right) \\ &\simeq B_2^{HS} \left( 1 - \frac{3}{2} (e^{U_S} - 1) \epsilon_0 \right), \end{aligned} \quad (26)$$

we thus identify

$$\frac{1}{\tau} \simeq 6\epsilon_0 (e^{U_S} - 1), \quad (27)$$

where  $U_S$  is given by Eq. (23). However, it is important to realize that this procedure is legitimate at small densities only. At finite concentrations, the optimal representation of the real suspension of proteins by a Baxter model has to be derived and we will show in section III that the simple-minded identification  $B_2^{AHS} \equiv B_2$  no longer applies.

## B. Application to lysozyme

### 1. Experimental Data

Lysozyme is, by far, the best studied protein with regard to solution properties. This is one of the reasons for using this protein to test theory, another being its moderate aspect ratio of about 1.5 so that it may be fairly well approximated by a sphere. Bovine Serum Albumin (BSA) has also been well studied, but is considerably more anisometric with an aspect ratio of about 3.5. Numerous measurements of the second virial coefficient of lysozyme have been published. In fact, there are quite a few sets of experiments pertinent to our analysis [14, 20, 21, 22, 23, 24, 25, 26, 27, 28].

It turns out that there is appreciable scatter in the data if we plot all measurements of  $B_2$  at a pH of about 4.5 as a function of ionic strength  $I$  (NaCl + small amount of Na acetate; we have set the ionic strength arising from the latter equal to  $0.6 \times$  concentration [21]) (see Fig. 2). Several sets of data [25, 28] appear to be way off the general curve within any reasonable margin of error. An important criterion is how well the  $\theta$  point (i.e. when  $B_2 = 0$ ) is established since then attractive forces—which we would like to understand—are well balanced against electrostatics—which we purportedly understand well. Experimentally speaking, it ought to be possible to monitor  $B_2$  accurately about the  $\theta$  point; large negative  $B_2$  values at  $I \gg I_\theta$  are more difficult to determine because the proteins may start to



aggregate or nucleate, in principle. Various polynomial fits for all data close to the  $\theta$  point yield  $I_\theta = 0.20 \pm 0.01$  M. Hence, we have regarded data sets [25, 28] markedly disagreeing with this ionic strength as anomalous so we have not taken them into consideration. Fig. 3 displays all data we have taken into account. Clearly, the composite curve yields a fairly reliable basis to test possible theories of the attractive force. On the other hand, it is unclear at present how the scatter in data in Fig. 2 translates into bounds for inferred attractive interactions.

## 2. Theory

### 2a. Electrostatics

Next, it is important to ascertain the actual and effective charges of lysozyme under conditions relevant to the present work. Kuehner et al [29] performed hydrogen-ion titrations on hen-egg-white lysozyme in KCl solutions. By interpolation, we obtain the actual charge  $Z$  of the protein as a function of the 1-1 electrolyte concentration  $I$  (see tables I and II). Experiments on  $B_2$  are usually carried out with NaCl (and some Na acetate) as the supporting monovalent electrolyte but we here assume KCl and NaCl behave identically in an electrostatic sense. We solve the Poisson-Boltzmann equation to get the effective charge  $Z_{eff}$  in the Debye-Hückel tail (for more detail, see Appendix A). The dimensionless radius is set equal to  $\mu = 3.28a\sqrt{I} = 5.58\sqrt{I}$  and Eq.(61) is used to compute the renormalized or effective charge. (Setting  $a = 1.7$  nm for lysozyme as in Refs. [20] and [23]; the Bjerrum length  $Q = 0.71$  nm for H<sub>2</sub>O at room temperature). The other dimensionless parameter is given by  $\xi = 0.209(\bar{Z}/(1 + \mu))^2$ , where  $\bar{Z} = Z_{eff} - 1$  (see below).

### 2b. Attractive well

We have assumed  $U_A$  and  $\delta$  to be independent of the ionic strength  $I$ . It is possible to show that this does not contradict the data displayed in Figs. 2 and 4. In Appendix B, we prove that if the interaction between the proteins is given by Eq. (3), then  $dB_2/d\mu < 0$  and  $d^2B_2/d\mu^2 > 0$ , the last inequality being valid if  $\xi < 1$ . We recall that  $\mu$  is proportional to  $\sqrt{I}$  so that Figs. 3 and 4 indeed bear out these inequalities after due rearrangement.

Next, we determine the optimal values of  $U_A$  and  $\delta$  yielding exact, numerical  $B_2(I)$  curves given by Eq. (5) which are the best fits to the data of Fig. 3. We require that  $I_\theta = 0.20 \pm 0.01$  is predicted absolutely which fixes  $U_A$ , say, and  $\delta$  is then determined by a nonlinear minimization procedure. We thus obtain  $U_A = 1.70 \pm 0.25$  and  $\delta = 0.468 \mp 0.097$  but we note that the quantity  $\delta \exp U_A = 2.56 \pm 0.10$  is much more narrowly bounded. Now, it can be argued that the Debye-Hückel potential with effective charge  $Z_{eff}$  overestimates the real potential in magnitude so we have repeated this numerical procedure with a slightly lower effective charge, viz.  $\bar{Z} = Z_{eff} - 1$  (see tables I and II). This yields the revised estimates  $U_A = 2.87 \pm 0.65$ ,  $\delta = 0.167 \mp 0.086$  and  $\delta \exp U_A = 2.95 \pm 0.21$ . The numerically computed curves are displayed in Fig. 3. We therefore conclude that the variables  $U_A$  and  $\delta$  as such are difficult to ascertain unambiguously, though the variable  $\delta \exp U_A$  is quite robust. This is also borne out if we use our approximations, Eqs. (9) and (10), instead of the exact numerical computations. There are again wide variations in  $U_A$  and  $\delta$  but the quantity  $\delta \exp U_A$  is strictly bounded:  $\delta \exp U_A = 2.70 \pm 0.11$  (effective charge =  $Z_{eff}$ ) and  $\delta \exp U_A = 3.02 \pm 0.21$  (effective charge =  $Z_{eff} - 1$ ).

We now argue why  $\delta \exp U_A$  is indeed a relevant quantity, to a good approximation. At the  $\theta$  point we have  $B_2 = 0$  so that  $J_\theta = -8/3$  from Eq. (5). From tables I and II, we see that generally  $\mu \gg 1$  and  $\alpha\xi \ll 1$ ; hence, we have  $J_1 \simeq 4\xi/\mu$  and  $J_2 \simeq 4\delta \exp -\xi$  for often  $\mu\delta > 1$ . This would lead to  $\delta \exp U_A \simeq 4.4$ . On the other hand, at very high  $I$ ,  $J_1$  and  $\xi$  tend to zero and, because  $U_A \gg 1$ , the scaled virial coefficient  $B_2/B_2^{HS}$  reduces to  $-\frac{3}{8}J_2 \exp U_A \simeq -\frac{3}{2}\delta \exp U_A$  leading to  $\delta \exp U_A \simeq 3$  estimated from Fig. 3. Hence, the two estimates at the respective extremes are fairly consistent. To summarize, we may propose a crude approximation to the second virial coefficient which is a universal function of  $\delta \exp U_A$

$$\frac{B_2}{B_2^{HS}} \simeq 1 + \frac{3\xi}{2\mu} - \frac{3}{2}e^{-\xi}\delta e^{U_A}. \quad (28)$$

The third term on the right is exact in the limit  $\delta \rightarrow 0$ , whereas the absolute error in the second term is smaller than 0.25 when  $I \geq 0.1$  M. Using Eq. (28) to fit the data leads to  $\delta \exp U_A = 4.2$  when we use the effective charge  $Z_{eff}$ , whereas  $\delta \exp U_A = 3.7$  when we use the lower effective charge  $\bar{Z}$  (see Fig. 5).

In Fig. 3 we see that the curves at low values of  $\delta$  fit the data at high ionic strengths better. In the remainder of this article, we therefore employ the values  $\delta = 0.079$  and  $U_A = 3.70$ , corresponding to the lowered effective charge  $\bar{Z}$  and  $I_\theta = 0.21$  M. In Fig. 6 we

show a comparison between the experimental data at a pH of about 7.5 and the theoretical curve computed numerically with the same parameters.

### 3. AHS potential

Values of  $\epsilon_0$ ,  $U_S$  and  $\tau$  at several ionic strengths are given in tables I and II. Fig. 7 displays the ionic-strength dependence of the adhesion parameter  $\tau$ . Near the  $\theta$  point,  $\tau$  decreases quickly with increasing  $I$ . At high ionic strength,  $\tau$  approaches the limiting value of  $(6\delta(e^{U_A} - 1))^{-1}$ , which, upon the use of our choice  $\delta = 0.079$  and  $U_A = 3.7$ , is equal to 0.0535. We note that at pH 4.5 and at ionic strengths  $I = 0.05$  M and  $I = 0.1$  M, the computed values of  $\epsilon_0$ ,  $U_S$  and  $\tau$  become nonsensical. In that case, the attractive potential is simply not strong enough to compensate the electrostatic repulsion completely so our analytical approach breaks down. This can also be seen in Fig. 2, where we have  $B_2 > B_2^{HS}$  for these two values of the ionic strength. The same effect occurs at pH 7.5 when  $I = 0.05$  M.

## III. LIQUID STATE THEORY AT HIGHER DENSITIES

### A. Theory

#### 1. Density dependent attractive well in the Baxter limit

In section II, we introduced the AHS potential as a convenient first approximation to the interaction between proteins. We determined the adhesion parameter  $\tau$  by matching values of the second virial coefficient which is methodologically correct only in the asymptotic limit of very low densities. In this section we propose a new procedure of choosing  $\tau$ , which is valid at higher densities but  $\tau$  now depends on the protein density. We extend a method originally proposed by Weeks, Chandler and Anderson [30] for repulsive interactions. They variationally determined an effective hard sphere diameter for a soft, repulsive potential of short-range, but we argue that their scheme is more generally applicable as long as the full interaction remains of short range, which is the case here.

We start by introducing a functional expansion of the excess Helmholtz free energy  $\Delta A$

in terms of the Mayer function of the interaction  $U$

$$\begin{aligned} \rho^{-1}\mathcal{A}(\rho, T; \varphi_s) &= \rho^{-1}\mathcal{A}(\rho, T; \varphi_{AHS}) + \frac{\eta}{2} \frac{3}{4\pi} \int d\mathbf{x} B_{AHS}(x) + \\ &+ \frac{\eta^2}{2} \left(\frac{3}{4\pi}\right)^2 \frac{a^3}{V} \int d\mathbf{x}_1 d\mathbf{x}_2 d\mathbf{x}_3 B_{AHS}(x_{12}) B_{AHS}(x_{13}) J_{AHS}^{(3)}(\mathbf{x}_1, \mathbf{x}_2, \mathbf{x}_3) + \dots \end{aligned} \quad (29)$$

Here,  $V$  is the volume of the system,  $\mathcal{A} = -\Delta A/V$ ,  $\varphi_s(x) = e^{-U(x)}$ ,  $\varphi_{AHS}(x) = e^{-U_{AHS}(x)}$ ,  $\eta = 4\pi a^3 \rho/3$  is the volume fraction of particles,  $J_{AHS}^{(3)}(\mathbf{x}_1, \mathbf{x}_2, \mathbf{x}_3)$  is a complicated function depending on two and three particle correlation functions (see [30]) and  $\mathbf{x}_{12} = \mathbf{x}_1 - \mathbf{x}_2$  etc. We define the quantity

$$B_{AHS}(x) \equiv y_{AHS}(x) [\varphi_s(x) - \varphi_{AHS}(x)], \quad (30)$$

in terms of the so-called cavity function  $y_{AHS}(x) \equiv g_{AHS}(x)/\varphi_{AHS}(x) = \frac{2}{\rho^2} \frac{\delta \mathcal{A}}{\delta \varphi(x)}$  and radial distribution function  $g_{AHS}(x)$  pertaining to an appropriate AHS potential which is the reference state. Both these functions depend on  $\rho$ ,  $T$  and the effective adhesive parameter  $\tau$ , the latter to be determined variationally. From now on, we omit the subscript  $AHS$  in  $B_{AHS}(x)$ ,  $g_{AHS}(x)$  etc. for the sake of brevity.

We next choose  $\tau$  by requiring that the first-order correction to the excess free energy vanishes

$$\int d\mathbf{x} B(x) = 0. \quad (31)$$

This is the analogue of Eq. (12). Hence, in the spirit of the previous section, we split up this integral into two parts. The first indicates that the tail of the electrostatic interaction is compensated by part of the original square well attraction

$$\int_{2+\epsilon}^{\infty} dx x^2 B(x) = 0 \quad (32)$$

( $0 < \epsilon \leq \delta$ ) and yields  $\epsilon$ . The second determines the density dependent strength  $\tau$  of the AHS interaction

$$\int_2^{2+\epsilon} dx x^2 B(x) = 0. \quad (33)$$

This expresses the fact that the reference potential has to compensate for the remaining part of the original interaction.

## 2. Approximate radial distribution function for the Baxter potential

In order to be able to determine  $\tau$  from Eqs. (32) and (33), we need to know  $g(x)$ , the radial distribution function of the reference interaction, the AHS potential. In the Percus-Yevick approximation developed by Baxter,  $g(x)$  has a singular contribution  $g_\omega(x)$  which, after the limit  $\omega \rightarrow 0$ , acts like a delta function and results from the stickiness of the interaction at the surfaces of two touching spheres. We split  $g(x)$  into  $g_\omega(x)$  and a regular term  $\tilde{g}(x)$  [19]

$$g(x) = \tilde{g}(x) + g_\omega(x) \quad (34)$$

with

$$g_\omega(x) = \begin{cases} 0 & x < 2 \\ \frac{\lambda(2+\omega)}{12\omega} + O(1) & 2 \leq x \leq 2 + \omega \\ 0 & x > 2 + \omega \end{cases} \quad (35)$$

analogously to Eq. (24), where the amplitude  $\lambda$  is the smaller of the two solutions of

$$\tau = \frac{1 + \eta/2}{(1 - \eta)^2} \frac{1}{\lambda} - \frac{\eta}{1 - \eta} + \frac{\eta}{12} \lambda. \quad (36)$$

For  $x < 2$ ,  $\tilde{g}(x)$  equals zero owing to the hard-core repulsion, whereas  $\tilde{g}(x)$  tends to unity for large  $x$ . For proteins, it turns out that  $\varphi_s(x) - \varphi_{AHS}(x)$  is often appreciably nonzero only near the surface of the sphere so we approximate  $\tilde{g}(x)$  in the interval  $2 \leq x \leq 4$  by the first two terms of its Taylor expansion

$$\tilde{g}(x) \simeq \begin{cases} 0 & x < 2 \\ G(1 + H(x - 2)) & 2 \leq x \leq 4 \\ 1 & x > 4 \end{cases}, \quad (37)$$

The two constants have been derived by Bravo Yuste and Santos [31]

$$G = \lambda\tau \quad (38)$$

and

$$H = \frac{\eta}{2\tau(1 - \eta)} \left( \frac{\eta(1 - \eta)}{12} \lambda^2 - \frac{1 + 11\eta}{12} \lambda + \frac{1 + 5\eta}{1 - \eta} - \frac{9(1 + \eta)}{2(1 - \eta)^2} \frac{1}{\lambda} \right). \quad (39)$$

Numerical work [32] bears out that Eq. (37) is quite reasonable since the range of both attractive and electrostatic forces is much smaller than the diameter of the protein.

### 3. Determination of the effective adhesion

We next determine  $\tau$  from Eq. (33), first using Eq. (32) to obtain  $\epsilon$ . From Eqs. (24), (30) and (34), the function  $B(x)$  can be shown to have the following form (repressing terms that ultimately disappear in the limit  $\omega \rightarrow 0$ )

$$B(x) = \tilde{B}(x) - g_\omega(x), \quad (40)$$

where the regular term is given by

$$\tilde{B}(x) = \begin{cases} 0 & 0 \leq x \leq 2 \\ (e^{-U(x)} - 1)\tilde{g}(x) & x > 2 \end{cases}. \quad (41)$$

Eq. (32) may be conveniently expressed as

$$\int_{2+\epsilon}^{\infty} dx x^2 B(x) = \int_{2+\epsilon}^{2+\delta} dx x^2 \tilde{B}(x) + \int_{2+\delta}^{\infty} dx x^2 \tilde{B}(x) = 0. \quad (42)$$

Using  $\int_{2+\epsilon}^{2+\delta} dx f(x) \simeq \frac{1}{2}(\delta - \epsilon) [f(2 + \delta) + f(2 + \epsilon)]$  and neglecting terms of order  $\delta^2$  and  $\epsilon^2$ , we write the first integral as

$$\int_{2+\epsilon}^{2+\delta} dx x^2 B(x) \simeq G(\delta - \epsilon)K_1(\delta, \epsilon), \quad (43)$$

with

$$K_1(\delta, \epsilon) \equiv 2 \left( e^{U_A} e^{-\frac{\xi}{1+\delta/2} e^{-\mu\delta}} - 1 \right) (1 + (1 + H)\delta) + 2 \left( e^{U_A} e^{-\frac{\xi}{1+\epsilon/2} e^{-\mu\epsilon}} - 1 \right) (1 + (1 + H)\epsilon). \quad (44)$$

Again, we stress that, although  $\delta \ll 1$  and  $\epsilon \ll 1$ ,  $\mu\delta$  and  $\mu\epsilon$  may be of order unity. Furthermore, we note that if we take the limit  $\eta \downarrow 0$ , then  $\lambda \rightarrow \tau^{-1}$  and  $G \rightarrow 1$ , so we recover Eq. (16) if we neglect terms of order  $\delta$  and  $\epsilon$ . We tackle the second integral by adopting the approximation:  $1 - \exp(-U(x)) = 1 - \exp(2\xi x^{-1} e^{-\mu(x-2)}) \simeq 2\xi x^{-1} e^{-\mu(x-2)} - 2\xi^2 x^{-2} e^{-2\mu(x-2)} + 2\xi^3 x^{-2} e^{-3\mu(x-2)}/3$  (note that in this Taylor expansion of the exponential we have replaced one factor  $x^{-1}$  by  $2^{-1}$  in the last term). We then write

$$- \int_{2+\delta}^{\infty} dx x^2 B(x) \simeq G((1 + \delta H)P_1 + HP_2) \quad (45)$$

with

$$P_1 = \int_{2+\delta}^{\infty} dx x^2 (1 - e^{-U(x)}) \simeq \frac{8}{\mu^2} (1 + \mu\delta)M + \frac{16}{\mu} M \left( 1 - M + \frac{8}{9}M^2 \right) \quad (46)$$

and

$$P_2 = \int_{2+\delta}^{\infty} dx x^2 (x-2-\delta)(1-e^{-U(x)}) \simeq \frac{8}{\mu^3} (2+\mu\delta)M + \frac{16}{\mu^2} \left( M - \frac{1}{2}M^2 + \frac{8}{27}M^3 \right). \quad (47)$$

Here,  $M \equiv \xi e^{-\mu\delta}/4$ . Using the approximations  $1-M+8M/9 \simeq (1+M)^{-1}$  and  $M-M^2/2+8M^3/27 \simeq \log(1+M)$ , we arrive at

$$P_1 \simeq \frac{8}{\mu^2} (1+\mu\delta)M + \frac{16}{\mu} \frac{M}{1+M} \quad (48)$$

and

$$P_2 \simeq \frac{8}{\mu^3} (2+\mu\delta)M + \frac{16}{\mu^2} \log(1+M). \quad (49)$$

Hence, the variable  $\epsilon$ , which depends on the density by virtue of the density dependence of  $G$  and  $H$ , is determined iteratively from

$$\delta - \epsilon_{new} = \frac{(1+\delta H)P_1 + HP_2}{K_1(\delta, \epsilon_{old})}. \quad (50)$$

One starts with  $\epsilon_{old} = \delta$  and iterates until a stationary  $\epsilon_{new}$  is reached.

The next step is to calculate  $\tau$  from Eq. (33), which, with the help of Eq. (40), is equivalent to the expression

$$\int_2^{2+\epsilon} dx x^2 \tilde{B}(x) = \frac{2\lambda}{3}. \quad (51)$$

We have taken the limit  $\omega \rightarrow 0$ . Again using the approximation  $\int_2^{2+\epsilon} dx f(x) \simeq \frac{1}{2}\epsilon [f(2+\epsilon) + f(2)]$ , we write

$$\int_2^{2+\epsilon} dx x^2 \tilde{B}(x) \simeq 2G\epsilon \left[ \left( e^{U_A} e^{-\frac{\xi}{1+\epsilon/2} e^{-\mu\epsilon}} - 1 \right) (1 + (1+H)\epsilon) + (e^{U_A} e^{-\xi} - 1) \right]. \quad (52)$$

Together with the expressions Eq. (51) and  $G = \lambda\tau$  (Eq. (38)), this leads to

$$\frac{1}{\tau} \simeq 3\epsilon \left[ \left( e^{U_A} e^{-\frac{\xi}{1+\epsilon/2} e^{-\mu\epsilon}} - 1 \right) (1 + (1+H)\epsilon) + (e^{U_A} e^{-\xi} - 1) \right]. \quad (53)$$

Accordingly,  $\tau$  may be determined iteratively if we recall that both  $H$  and  $\epsilon$  also depend on  $\tau$ . A way of quickly determining  $\tau$  and  $\epsilon$  is choosing a starting value for both ( $\epsilon = \delta$  and  $\tau = 0.2$  say), and then alternately using Eqs. (50) and (53) until the iterates become stationary.

## B. Application to lysozyme

We have already determined the interaction in section IIB2b. We next compute  $\tau$  iteratively and it now depends on both the density of protein and the ionic strength. (See table III).

Thermodynamic properties like the osmotic compressibility  $\kappa_T$  are also simply obtained from  $\tau$ . In the Percus-Yevick approximation,  $\kappa_T$  is given by [19]

$$(\rho k_B T \kappa_T)^{-1} \equiv \frac{1}{k_B T} \frac{\partial \Pi}{\partial \rho} = \frac{(1 + 2\eta - \lambda\eta(1 - \eta))^2}{(1 - \eta)^4}, \quad (54)$$

where  $\lambda$  is the smaller of the two solutions of Eq. (36). Fig. 8 compares the predicted density dependence of the (scaled) inverse osmotic compressibility at various ionic strengths with experimental data from [13] and [14].

## IV. DISCUSSION

One difficulty in comparing our computations with experiment has been the substantial margin of error in the osmotic measurements. In the case of other biomacromolecules like rodlike DNA, it has been possible to obtain the second virial  $B_2$  at better than 10% accuracy [33, 34, 35]. One possibility for the occurrence of discrepancies in  $B_2$  is the variety of lysozyme types. Poznanski et al [36] have established that popular commercial lysozyme preparations like Seikagaku and Sigma exhibit significant differences under dynamic light scattering. Nevertheless, the variation in  $B_2$  at, say, about 0.5 M NaCl (see Fig. 3), is so large that it needs to be explained.

The relatively large variation in the experimental measurements of  $B_2$  makes it difficult to falsify stringently other models of attractive forces like that of van der Waals type, for instance. It proves feasible to get satisfactory agreement with the experimental data displayed in Fig. 3 if we let the dispersion interaction be given by the nonretarded Hamaker potential [18] for spheres of dimensions appropriate for lysozyme, with an adjustable Hamaker constant of order  $k_B T$  though with a very short cut-off at around 0.1 – 0.2 nm. However, the necessity of such a cut-off, which is already beyond the limit of validity of continuum approximations, may be viewed as positing the equivalent of a short-range interaction like that of Eq. (3), in large part. The long-range dispersion interaction beyond some distance



much smaller than the radius  $a$ , plays only a minor role.

Stell [37] has criticized the Baxter limit because divergences in the free energy appear at the level of the 12th virial. Therefore, the most straightforward way to interpret our liquid state theory is to stress that our zero-order theory describes the reference state only up to and including the 11th virial within the Percus-Yevick approximation. The analysis of phase transitions must be viewed with caution (for a comparison of recent simulations—taking the limit of zero polydispersity after the limit of vanishing well depth—with Percus-Yevick theory, see [38]). A second problem is here that, at large ionic strengths, a considerable electrostatic repulsion is balanced against a significant attraction (see Fig. 1) and it is difficult to see how good such a compensatory scheme should work at high concentrations near dense packing.

In summary, we have presented a fairly good theory of the ionic-strength dependence of the osmotic properties of lysozyme in terms of a sticky interaction which is independent of charge or salt concentration. This conclusion, by itself, is not new for it has been reached earlier by formulating numerical work incorporating short-range forces and screened electrostatics and comparing it with X-ray scattering [39, 40] and liquid-liquid phase separation [41, 42, 43]. The merit of the current analysis is its transparency because it is analytical and it is based on a nonperturbative variational principle for general short-range potentials so it may be readily generalized.

## V. APPENDIX

### A. Effective charge

For the repulsive tail of the two particle interaction, we use the Debye-Hückel potential, which is the far-field solution of the Poisson-Boltzmann equation. In our case, the (dimensionless) potential at the surface is often merely of order unity, so the Debye-Hückel potential slightly overestimates the solution to the Poisson-Boltzmann equation. To remedy this, we use a renormalized charge within the Debye-Hückel potential, chosen in such a way that, at large distances, the Debye-Hückel potential coincides with the tail of the solution of the Poisson-Boltzmann equation determined by the real charge [44]. This will result in an underestimation of the potential at small separations, but the form of the Debye-Hückel

potential we use here (Eq. (4)) is in fact only accurate at large separations and overestimates the interaction at small separations appreciably i.e. when overlap of the two double layers occurs (by about 20%, see [18]). The two effects thus partly cancel, although the latter effect is larger than the former.

The Poisson-Boltzmann equation for the dimensionless potential  $\psi(r) = q\phi(r)/k_B T$  of a single sphere of radius  $a$  and total charge  $qZ$ , assumed positive for convenience, immersed in a solvent with Bjerrum length  $Q$ , at a concentration of ions leading to a Debye length  $\kappa$ , is written as

$$\frac{1}{r^2} \frac{d}{dr} r^2 \frac{d}{dr} \psi(r) = \kappa^2 \sinh \psi(r), \quad (55)$$

with boundary conditions

$$\left. \frac{d}{dr} \psi(r) \right|_{r=a} = \frac{ZQ}{a^2}; \quad \lim_{r \rightarrow \infty} \psi(r) = 0. \quad (56)$$

Linearizing Eq. (55) ( $\psi \ll 1$ ), we find the Debye-Hückel solution

$$\psi_0 = \frac{ZQ}{1+\mu} \frac{e^{-\kappa(r-a)}}{r}. \quad (57)$$

We next derive the first-order correction to this solution. Putting  $\psi(r) = \psi_0(r) + \psi_1(r)$ , with  $|\psi_1(r)| \ll |\psi_0(r)|$ , results in the following linear differential equation for  $\psi_1$

$$\frac{1}{r^2} \frac{d}{dr} r^2 \frac{d}{dr} \psi_1(r) = \frac{1}{6} \kappa^2 \psi_0^3(r). \quad (58)$$

Keeping in mind that  $\psi_1(r) = o(\psi_0(r))$ , as  $r \rightarrow \infty$ , we integrate the differential equation once to obtain

$$\frac{d}{dr} \psi_1(r) = -\frac{\kappa^2}{6} \left( \frac{ZQe^\mu}{1+\mu} \right)^3 \frac{E_1(3\kappa r)}{r^2} \quad (59)$$

and a second time to derive

$$\psi_1(r) = -\frac{\kappa^3}{6} \left( \frac{ZQe^\mu}{1+\mu} \right)^3 \left( \frac{e^{-3\kappa r}}{\kappa r} - \left( 3 + \frac{1}{\kappa r} \right) E_1(3\kappa r) \right), \quad (60)$$

where  $E_1(x)$  is the exponential integral defined by  $E_1(x) = \int_x^\infty dt t^{-1} e^{-t}$ . Using the first of the two boundary conditions, we then determine the renormalized charge  $Z_{eff}$

$$\begin{aligned} Z_{eff} &= \frac{a^2}{Q} \left. \frac{d}{dr} \psi(r) \right|_{r=a} = \frac{a^2}{Q} \left. \frac{d}{dr} \psi_0(r) \right|_{r=a} + \frac{a^2}{Q} \left. \frac{d}{dr} \psi_1(r) \right|_{r=a} = \\ &= Z - \frac{\mu}{18} \left( \frac{Q}{a} \right)^2 \left( \frac{Z}{1+\mu} \right)^3 F(\mu), \end{aligned} \quad (61)$$

where

$$F(\mu) \equiv 3\mu e^{3\mu} E_1(3\mu) \sim 1 - \frac{1}{3\mu} + \frac{2}{9\mu^2} - \dots \quad (62)$$

Recapitulating, we have calculated, to leading order, the charge  $Z_{eff}$  which has to be inserted into the Debye-Hückel potential (Eq. (4)) so that this has the correct asymptotic behavior at large  $r$ , coinciding with the tail of the Poisson-Boltzmann solution.

### B. Dependence of $B_2$ on ionic strength

Here, we prove some simple inequalities describing the behavior of the second virial coefficient as a function of the ionic strength for an interaction consisting of a Debye-Hückel repulsion  $U_{DH}(x)$  and a general attractive potential  $U_A(x)$ , the latter not depending on the ionic strength. If we let  $U(x) = U_{DH}(x) + U_A(x)$ , then  $B_2$  is given by Eq. (5) with

$$J = \int_2^\infty dx x^2 (1 - e^{-U(x)}). \quad (63)$$

Then, we have

$$\frac{dJ}{d\mu} = \int_2^\infty dx x^2 \frac{dU_{DH}(x)}{d\mu} e^{-U(x)} = \int_2^\infty dx x^2 \left( \frac{d \ln \xi}{d\mu} - (x-2) \right) U_{DH}(x) e^{-U(x)}. \quad (64)$$

In Fig. 9 we see that in the regime of interest  $\frac{d \ln \xi}{d\mu} < 0$ , so we conclude that

$$\frac{dB_2}{d\mu} = \frac{3}{8} B_2^{HS} \frac{dJ}{d\mu} < 0. \quad (65)$$

In the same way it is clear from the second derivative

$$\frac{d^2 J}{d\mu^2} = \int_2^\infty dx x^2 \left( \frac{d^2 \ln \xi}{d\mu^2} + \left( \frac{d \ln \xi}{d\mu} - (x-2) \right)^2 (1 - U_{DH}(x)) \right) U_{DH}(x) e^{-U(x)} \quad (66)$$

and the fact that  $\frac{d^2 \ln \xi}{d\mu^2} \gtrsim 0$  in the regime of interest, that

$$\frac{d^2 B_2}{d\mu^2} = \frac{3}{8} B_2^{HS} \frac{d^2 J}{d\mu^2} > 0, \quad (67)$$

if  $U_{DH}(2) < 1$ , i.e. if  $\xi < 1$  (a sufficient condition).

### C. Corrections to the free energy

In section III, we viewed a suspension of proteins as a system of spheres with an AHS interaction and we chose the parameter  $\tau$  of the AHS potential such that the first order

correction in the functional expansion of the free energy (Eq. (29)) vanishes (see Eq. (31)). In an attempt to justify this approximation and explore its regime of applicability, we estimate the size of the second order correction to the free energy (from Eq. (29)) which is either positive or negative definite

$$\Delta \equiv \frac{\eta^2}{2} \left( \frac{3}{4\pi} \right)^2 a^3 V^{-1} \int d\mathbf{x}_1 d\mathbf{x}_2 d\mathbf{x}_3 B(x_{12})B(x_{13})h(x_{23}) = \frac{9}{4}\eta^2 Y. \quad (68)$$

It is convenient to rewrite the integral in such a way that the angular integration can be performed explicitly (see below).

$$\begin{aligned} Y &\equiv \int_0^\infty dt t^2 B(t) \int_0^\infty ds s^2 B(s) \int_0^\pi d\vartheta \sin \vartheta h(\sqrt{s^2 + t^2 - 2st \cos \vartheta}) = \\ &= 2 \int_0^\infty dt t B(t) \int_t^\infty ds s B(s) \int_{s-t}^{s+t} du u h(u). \end{aligned} \quad (69)$$

Here we have used the Kirkwood superposition approximation  $J_{BM}^{(3)}(\mathbf{x}_1, \mathbf{x}_2, \mathbf{x}_3) = h(x_{23})$  [30], where  $h(x) = g(x) - 1$  is the pair correlation function. We have employed the substitution  $u^2 = s^2 + t^2 - 2st \cos \vartheta$ , with  $\vartheta$  the angle between  $\mathbf{x}_{12}$  and  $\mathbf{x}_{13}$ . Using the expression for  $g(x)$  (Eq. (34)) and defining  $\tilde{h}(x) = \tilde{g}(x) - 1$ , we split  $Y$  into three parts

$$Y = Y_0 + Y_1 + Y_2 \quad (70)$$

where we have introduced the limit  $\omega \rightarrow 0$  and where

$$\begin{aligned} Y_0 &\equiv \frac{2\lambda}{3} \int_2^\infty dt t B(t) \int_t^{t+2} ds s B(s) \simeq \\ &\simeq \frac{2\lambda}{3} \int_2^\infty dt t B(t) \int_t^\infty ds s B(s) = \frac{\lambda}{3} \left[ \int_2^\infty dt t B(t) \right]^2, \end{aligned} \quad (71)$$

$$Y_1 \equiv 2 \int_2^\infty dt t B(t) \int_t^{t+2} ds s B(s) \int_{s-t}^{s+t} du u \tilde{h}(u). \quad (72)$$

and

$$Y_2 \equiv 2 \int_2^\infty dt t B(t) \int_{t+2}^{t+4} ds s B(s) \int_{s-t}^{s+t} du u \tilde{h}(u) \ll Y_1 \quad (73)$$

To simplify Eq. (72), we substitute Eq. (37) and note that  $s + t \geq 4$  and  $0 \leq s - t \leq 2$ . We then derive

$$\int_{s-t}^{s+t} du u \tilde{h}(u) = \frac{2}{3} (9G + 10GH - 12) + \frac{1}{2} (s - t)^2. \quad (74)$$

Next, using Eq. (31), we integrate the nonconstant term leading to a product of two integrals

$$\begin{aligned} \int_2^\infty dt tB(t) \int_t^{t+2} ds sB(s)(s-t)^2 &\simeq \int_2^\infty dt tB(t) \int_t^\infty ds sB(s)(s-t)^2 = \\ &= \left[ \int_2^\infty dt tB(t) \right] \left[ \int_2^\infty ds s^3B(s) \right]. \end{aligned} \quad (75)$$

Hence,  $Y_1$  is written in terms of one-dimensional integrals

$$Y_1 \simeq \frac{2}{3} (9G + 10GH - 12) \left[ \int_2^\infty dt tB(t) \right]^2 + \left[ \int_2^\infty dt tB(t) \right] \left[ \int_2^\infty ds s^3B(s) \right], \quad (76)$$

and this is also the case for  $Y$

$$Y \simeq \frac{2}{3} \left( 9G + 10GH - 12 + \frac{\lambda}{2} \right) \left[ \int_2^\infty dt tB(t) \right]^2 + \left[ \int_2^\infty dt tB(t) \right] \left[ \int_2^\infty ds s^3B(s) \right]. \quad (77)$$

Our goal is to obtain explicit approximations for these integrals by expediently using Eqs. (32) and (33). First, we consider integrals on the interval  $[2, 2 + \epsilon]$  which are dominated by the singular part of  $B(x)$ . We substitute Eq. (40) into (33) and let  $\omega \rightarrow 0$

$$\int_2^{2+\epsilon} dt t^2 \tilde{B}(t) = \frac{2\lambda}{3}. \quad (78)$$

We use this relation to rewrite part of one of the integrals in Eq. (77) in two ways, noting that  $\epsilon \ll 1$ .

$$\int_2^{2+\epsilon} dt tB(t) = -\frac{\lambda}{3} + \int_2^{2+\epsilon} dt t\tilde{B}(t) = -\frac{1}{2} \int_2^{2+\epsilon} dt (t-2)t\tilde{B}(t) \simeq -\frac{\epsilon}{4} \int_2^{2+\epsilon} dt t\tilde{B}(t). \quad (79)$$

We thus conclude that

$$\int_2^{2+\epsilon} dt t\tilde{B}(t) \simeq \left( 1 - \frac{\epsilon}{4} \right) \frac{\lambda}{3} \quad (80)$$

so the first equality in Eq. (79) allows us to attain the explicit expression

$$\int_2^{2+\epsilon} dt tB(t) \simeq -\frac{\lambda\epsilon}{12}. \quad (81)$$

Similarly, we use Eqs. (40) and (78) to evaluate part of the other integral in Eq. (77).

$$\int_2^{2+\epsilon} dt t^3B(t) = -\frac{4\lambda}{3} + \int_2^{2+\epsilon} dt t^3\tilde{B}(t) = \int_2^{2+\epsilon} dt (t-2)t^2\tilde{B}(t) \simeq \frac{\lambda\epsilon}{3}. \quad (82)$$

We note that both integrals in Eqs. (81) and (82) are  $O(\epsilon)$  because the integral in Eq. (78) is independent of  $\epsilon$  owing to the singular part of  $B(x)$ . If  $B(x)$  had been completely regular, the integrals in Eqs. (81) and (82) would have been  $O(\epsilon^2)$ .

We next consider the remaining two integrals on the interval  $[2 + \epsilon, \infty)$ . We start by splitting Eq. (32) into two parts since  $2 + \delta$  demarcates two different regimes

$$\int_{2+\epsilon}^{2+\delta} dt t^2 B(t) + \int_{2+\delta}^{\infty} dt t^2 B(t) = 0. \quad (83)$$

Using this equation and the approximation  $B(t) \simeq -2\xi e^{-\mu(t-2)}/t$ , we may simplify the two integrals, ultimately omitting  $O(\delta)$  terms

$$\begin{aligned} \int_{2+\epsilon}^{\infty} dt t B(t) &= \int_{2+\epsilon}^{2+\delta} dt t B(t) + \int_{2+\delta}^{\infty} dt t B(t) \simeq \\ &\simeq \frac{1}{2} \left(1 - \frac{\delta}{2}\right) \int_{2+\epsilon}^{2+\delta} dt t^2 B(t) + \int_{2+\delta}^{\infty} dt t B(t) = \\ &= \frac{\delta}{4} \int_{2+\delta}^{\infty} dt t^2 B(t) - \frac{1}{2} \int_{2+\delta}^{\infty} dt t(t-2) B(t) \simeq \frac{\xi}{\mu^2} e^{-\mu\delta} \end{aligned} \quad (84)$$

$$\begin{aligned} \int_{2+\epsilon}^{\infty} dt t^3 B(t) &= \int_{2+\epsilon}^{2+\delta} dt t^3 B(t) + \int_{2+\delta}^{\infty} dt t^3 B(t) = \\ &\simeq (2 + \delta) \int_{2+\epsilon}^{2+\delta} dt t^2 B(t) + \int_{2+\delta}^{\infty} dt t^3 B(t) = \\ &= -\delta \int_{2+\delta}^{\infty} dt t^2 B(t) + \int_{2+\delta}^{\infty} dt t^2(t-2) B(t) \simeq -4 \frac{\xi}{\mu^2} e^{-\mu\delta}. \end{aligned} \quad (85)$$

We remark that both expressions in Eqs. (84) and (85) are  $O(\mu^{-2})$  because  $B(t)$  is regular for  $t \geq 2 + \epsilon$ . We then combine Eqs. (81) and (84), and Eqs. (82) and (85)

$$\int_2^{\infty} dt t B(t) \simeq -\frac{\lambda\epsilon}{12} + \frac{\xi}{\mu^2} e^{-\mu\delta} \simeq -\frac{1}{4} \int_2^{\infty} ds s^3 B(s). \quad (86)$$

Finally, using Eqs. (68), (77) and (86), we arrive at an approximation for the correction to the free energy

$$\Delta = \frac{9}{4} \eta^2 Y \simeq \frac{9}{2} \eta^2 \left( G + H - 6 + \frac{\lambda}{6} \right) \left[ \frac{\xi}{\mu^2} e^{-\mu\delta} - \frac{\lambda\epsilon}{12} \right]^2. \quad (87)$$

Despite the variety of approximations used, this expression still retains its “definite” character (it turns out to be negative in the numerical calculations below). However, the numerical coefficients within the last quadratic factor are not exact. Furthermore, the status of the present theory differs from that of the Weeks-Chandler-Anderson theory [30]. In the latter,  $\Delta$  is of fourth order in the perturbation whereas it is basically quadratic here for the reason stated below Eq. (82).

To estimate the importance of this correction, we first calculate the osmotic pressure resulting from the neglect of second and higher order terms in the functional expansion Eq. (29). This amounts to determining  $\tau$  from Eqs. (36), (50) and (53) and then computing the osmotic pressure from Ref. [19]

$$\frac{\Pi}{\rho k_B T} = \frac{1 + \eta + \eta^2 - \lambda\eta(1 - \eta)(1 + \frac{1}{2}\eta) + \lambda^3\eta^2(1 - \eta)^3/36}{(1 - \eta)^3}. \quad (88)$$

Then, we evaluate the correction to the osmotic pressure due to the second order term in Eq. (29). The osmotic pressure is related to the free energy by

$$\frac{\Pi}{\rho k_B T} = -\eta \frac{\partial(\rho^{-1}\mathcal{A})}{\partial\eta}. \quad (89)$$

Because  $Y$  depends only weakly on  $\eta$ , we approximate the correction to the osmotic pressure by

$$-\eta \frac{\partial\Delta}{\partial\eta} \simeq -2\Delta. \quad (90)$$

We have compiled the pressure and its correction in table IV for the same sets of parameters as in table I (omitting the trivial case where  $\eta = 0$ ).

- 
- [1] A. George and W.W. Wilson, *Acta Crystallogr.* **D50**, 361 (1994).
  - [2] A. George, Y. Chiang, B. Guo, A. Arabshahi, Z. Cai and W.W. Wilson, *Methods Enzymol.* **276**, 100 (1997).
  - [3] M.H.J. Hagen and D. Frenkel, *J. Chem. Phys.* **101**, 4093 (1994).
  - [4] D. Rosenbaum, P.C. Zamora and C.F. Zukoski, *Phys. Rev. Lett* **76**, 150 (1996).
  - [5] C. Haas and J. Drenth, *J. Phys. Chem. B* **102**, 4226 (1998).
  - [6] C. Haas, J. Drenth and W.W. Wilson, *J. Phys. Chem. B* **103**, 2808 (1999).
  - [7] C. Haas and J. Drenth, *J. Cryst. Growth* **196**, 388 (1999).
  - [8] B.L. Neal, D. Asthagiri, O.D. Velev, A.M. Lenhoff and E.W. Kaler, *J. Cryst. Growth* **196**, 377 (1999).
  - [9] V.L. Vilker, C.K. Colton and K.A. Smith, *J. Coll. Int. Sci.* **79**, 548 (1981).
  - [10] A.P. Minton, *Biophys. Chem.* **57**, 65 (1995).
  - [11] B.M. Fine, A. Lomakin, O.O. Ogun and G.B. Benedek, *J. Chem. Phys.* **104**, 326 (1996).
  - [12] A. Lomakin, N. Asherie and G.B. Benedek, *J. Chem. Phys.* **104**, 1646 (1996).

- [13] R. Piazza, V. Peyre and V. Degiorgio, *Phys. Rev. E* **58**, R2733 (1998).
- [14] D.F. Rosenbaum, A. Kulkarni, S. Ramakrishnan and C.F. Zukoski, *J. Chem. Phys.* **111**, 9882 (1999).
- [15] A.J. Sophianopoulos, C.K. Rhodes, D.N. Holcomb and K.E. van Holde, *J. Biol. Chem.* **237**, 1107 (1962).
- [16] J.B. Keller and B. Zumino, *J. Chem. Phys.* **30**, 1351 (1959).
- [17] G.C. Maitland, V. Vesovic and W.A. Wakeham, *Mol. Phys.* **54**, 287 (1985).
- [18] E.J.W. Verwey and J. Th. G. Overbeek, *Theory of the Stability of Lyophobic Colloids* (Dover Publications, New York, 1999)
- [19] R.J. Baxter, *J. Chem. Phys.* **49**, 2770 (1968)
- [20] D.F. Rosenbaum and C.F. Zukoski, *J. Cryst. Growth* **169**, 752 (1996).
- [21] O.D. Velev, E.W. Kaler and A.M. Lenhoff, *Biophys. J.* **75**, 2682 (1998).
- [22] R.A. Curtis, J. Ulrich, A. Montaser, J.M. Prausnitz and H.W. Blanch, *Biotech. Bioeng.* **79**, 367 (2002).
- [23] R.A. Curtis, J.M. Prausnitz and H.W. Blanch, *Biotech. Bioeng.* **57**, 11 (1998).
- [24] M. Muschol and F. Rosenberger, *J. Chem. Phys.* **103**, 10424 (1995).
- [25] R. Piazza and M. Pierno, *J. Phys.: Condens. Matter* **12**, A443 (2000).
- [26] J. Bloustone, V. Berejnov and S. Fraden, *Biophys. J.* **85**, 2619 (2003).
- [27] F. Bonneté, S. Finet and A. Tardieu, *J. Cryst. Growth* **196**, 403 (1999).
- [28] J. Behlke and O. Ristau, *Biophys. Chem.* **76**, 13 (1999).
- [29] D.E. Kuehner, J. Engmann, F. Fergg, M. Wernick, H.W. Blanch and J.M. Prausnitz, *J. Phys. Chem. B* **103**, 1368 (1999).
- [30] J.D. Weeks, D. Chandler and H.C. Andersen, *J. Chem. Phys.* **54**, 5237 (1971); H.C. Andersen, J.D. Weeks and D. Chandler, *Phys. Rev. A* **4**, 1597 (1971); H.C. Andersen, D. Chandler and J.D. Weeks, *J. Chem. Phys.* **56**, 3812 (1972).
- [31] S. Bravo Yuste and A. Santos, *J. Stat. Phys.* **72**, 703 (1993).
- [32] W.G.T. Kranendonk and D. Frenkel, *Mol. Phys.* **64**, 403 (1988).
- [33] T. Nicolai and M. Mandel, *Macromolecules* **22**, 438 (1989).
- [34] M.E. Ferrari and V.A. Bloomfield, *Macromolecules* **25**, 5266 (1992).
- [35] P. Wissenburg, T. Odijk, P. Cirkel and M. Mandel, *Macromolecules* **28**, 2315 (1995).
- [36] J. Poznanski, Y. Georgalis, L. Wehr, W. Saenger and P. Zielenkiewicz, *Biophys. Chem.* **104**,



605 (2003).

- [37] G. Stell, *J. Stat. Phys.* **63**, 1203 (1991).
- [38] M.A. Miller and D. Frenkel, *Phys. Rev. Lett.* **90**, 135702 (2003).
- [39] M. Malfois, F. Bonneté, L. Belloni and A. Tardieu, *J. Chem. Phys.* **105**, 3290 (1996).
- [40] A. Tardieu, A. Le Verge, M. Malfois, F. Bonneté, S. Finet, M. Riès-Kautt and L. Belloni, *J. Cryst. Growth* **196**, 193 (1999).
- [41] V. Vlachy, H.W. Blanch and J.M. Prausnitz, *AIChE J.* **39**, 215 (1993).
- [42] J.J. Grigsby, H.W. Blanch and J.M. Prausnitz, *Biophys. Chem.* **91**, 231 (2001).
- [43] D.N. Petsev, X. Wu, O. Galkin and P.G. Vekilov, *J. Phys. Chem. B* **107**, 3921 (2003).
- [44] T.H. Gronwall, V.K. La Mer and K. Sandved, *Physik. Z.* **29**, 358 (1928).

## Tables

$I$ (M)	0.05	0.1	0.15	0.2	0.25	0.3	0.45	1	1.5	2
$Z$	9.5	9.8	10.0	10.1	10.2	10.2	10.3	10.4	10.4	10.4
$Z_{eff}$	8.8	9.2	9.4	9.6	9.7	9.8	10.0	10.2	10.3	10.3
$\bar{Z}$	7.8	8.2	8.4	8.6	8.7	8.8	9.0	9.2	9.3	9.3
$\xi$	2.52	1.84	1.48	1.27	1.10	0.984	0.752	0.409	0.295	0.229
$\mu$	1.25	1.76	2.16	2.50	2.79	3.06	3.74	5.58	6.83	7.89
$\epsilon_0$			0.0208	0.0466	0.0585	0.0644	0.0720	0.0773	0.0782	0.0785
$U_S$			2.26	2.52	2.70	2.82	3.05	3.37	3.47	3.53
$\tau$			0.933	0.314	0.205	0.164	0.115	0.0767	0.0684	0.0642

**Table I:** Values of the actual charge  $Z$  (from [29]), the renormalized or effective charge  $Z_{eff}$  (from Eq. (61)), the lowered effective charge  $\bar{Z} = Z_{eff} - 1$ , and dimensionless interaction parameters  $\xi$  and  $\mu$ , and  $\epsilon_0$ ,  $U_S$  and  $\tau$  as a function of the ionic strength  $I$ . The pH equals 4.5 and  $\xi$  has been calculated using the lowered effective charge  $\bar{Z}$ . Values of  $U_S$  and  $\tau$  have been computed using Eqs. (23) and (27), respectively, and  $\epsilon_0$  has been calculated using the procedure described immediately after Eq. (17).

$I$ (M)	0.05	0.1	0.15	0.2	0.25	0.3	0.45	1	1.5	2
$Z$	6.9	7.0	7.1	7.2	7.2	7.3	7.3	7.1	6.9	6.8
$Z_{eff}$	6.6	6.8	6.9	7.0	7.0	7.1	7.2	7.0	6.9	6.8
$\bar{Z}$	5.6	5.8	5.9	6.0	6.0	6.1	6.2	6.0	5.9	5.8
$\xi$	1.3	0.920	0.728	0.616	0.524	0.473	0.357	0.174	0.119	0.0889
$\mu$	1.25	1.76	2.16	2.50	2.79	3.06	3.74	5.58	6.83	7.89
$\epsilon_0$		0.0493	0.0640	0.0695	0.0725	0.0741	0.0764	0.0784	0.0787	0.0788
$U_S$		2.83	3.03	3.14	3.23	3.28	3.39	3.56	3.61	3.63
$\tau$		0.212	0.132	0.108	0.0943	0.0877	0.0758	0.0623	0.0590	0.0574

**Table II:** Same as table I, but now with a pH equal to 7.5.

$\eta$		0.15 M	0.2 M	0.25 M	0.3 M	0.45 M	1 M	1.5 M	2 M
0	$\tau$	0.829	0.295	0.194	0.156	0.110	0.0735	0.0656	0.0616
	$\epsilon$	0.0230	0.0483	0.0596	0.0653	0.0725	0.0775	0.0782	0.0786
0.05	$\tau$	0.712	0.289	0.193	0.155	0.110			
	$\epsilon$	0.0266	0.0492	0.0600	0.0655	0.0725			
0.1	$\tau$	0.620	0.283	0.192	0.155	0.110			
	$\epsilon$	0.0303	0.0502	0.0603	0.0656	0.0725			
0.15	$\tau$	0.544	0.276	0.191	0.155	0.110			
	$\epsilon$	0.0342	0.0514	0.0607	0.0657	0.0724			
0.2	$\tau$	0.482	0.268	0.190	0.155	0.110			
	$\epsilon$	0.0383	0.0528	0.0611	0.0658	0.0723			
0.3	$\tau$	0.380	0.251	0.186	0.154	0.110			
	$\epsilon$	0.0477	0.0563	0.0624	0.0663	0.0722			
0.4	$\tau$	0.300	0.228	0.179	0.152	0.110			
	$\epsilon$	0.0600	0.0619	0.0651	0.0677	0.0724			

**Table III:** The scaled depth  $\epsilon$  of the effective attractive well and the strength of the effective adhesive interaction  $\tau$  at pH 4.5 as a function of the ionic strength  $I$  and volume fraction  $\eta$ . The values of  $\epsilon$  and  $\tau$  have been evaluated from Eqs. (50) and (53)

$\eta$		0.15 M	0.2 M	0.25 M	0.3 M	0.45 M
0.05	$\frac{\Pi}{\rho k_B T}$	1.143	1.033	0.949	0.889	0.763
	$-2\Delta$	0.004	0.001	0.0004	0.0001	0.000008
0.1	$\frac{\Pi}{\rho k_B T}$	1.290	1.074	0.915	0.805	0.575
	$-2\Delta$	0.019	0.006	0.002	0.0005	0.00002
0.15	$\frac{\Pi}{\rho k_B T}$	1.437	1.123	0.898	0.749	0.448
	$-2\Delta$	0.044	0.014	0.004	0.001	0.00002
0.2	$\frac{\Pi}{\rho k_B T}$	1.583	1.183	0.904	0.721	0.375
	$-2\Delta$	0.085	0.026	0.008	0.003	0.000007
0.3	$\frac{\Pi}{\rho k_B T}$	1.866	1.361	0.988	0.753	0.340
	$-2\Delta$	0.228	0.068	0.022	0.008	0.00002
0.4	$\frac{\Pi}{\rho k_B T}$	2.17	1.659	1.231	0.960	0.470
	$-2\Delta$	0.488	0.143	0.046	0.016	0.0001

**Table IV:** The osmotic pressure from Eq. (88) and its correction from Eq. (90) as a function of the ionic strength  $I$  and the packing fraction  $\eta$ .

## Figure Captions

**Fig. 1:** The integrand of Eq. (2) versus the distance  $r$ . As shown by the shaded regions, the repulsive tail is compensated by part of the attractive interaction.

**Fig. 2:** Experimental data of the second virial coefficient  $B_2$  of lysozyme as a function of the ionic strength  $I$  at a pH of about 4.5. The second virial coefficient is scaled by the hard sphere value  $B_2^{HS}$ . Black squares: Bonneté et al. [27], pH 4.5, 20°C; grey triangles: Curtis et al. [23], pH 4.5, 20°C; grey squares: Muschol et al. [24], pH 4.7, 20°C; black stars: Curtis et al. [22], pH 4.5, 25°C; black diamonds: Bonneté et al. [27], pH 4.5, 25°C; black triangles: Velev et al. [21], pH 4.5, 25°C; white squares: Rosenbaum et al. [20], pH 4.6, 25°C; white diamonds: Rosenbaum et al. [14], pH 4.6, 25°C; grey stars: Bloustine et al. [26], pH 4.6, 25°C; white stars: Piazza et al. [25], pH 4.7, 25°C; white triangles: Behlke et al. [28], pH 4.5; grey diamonds: Bloustine et al. [26], pH 4.7. In all cases, the electrolyte is NaCl, often with a small amount of Na acetate added.

**Fig. 3:** A fit of Eq. 5 to the experimental data of Fig. 2 (except for those of Refs. [25] and [28]). On the right-hand side of the figure, the upper solid line corresponds to  $I_\theta = 0.19$ ,  $\delta = 0.564$  and  $U_A = 1.48$ , the upper dotted line to  $I_\theta = 0.20$ ,  $\delta = 0.468$  and  $U_A = 1.70$  and the middle solid line to  $I_\theta = 0.21$ ,  $\delta = 0.379$  and  $U_A = 1.95$ , all at an effective charge  $Z_{eff}$ . The middle dotted line corresponds to  $I_\theta = 0.19$ ,  $\delta = 0.25$  and  $U_A = 2.4$ , the lower solid one to  $I_\theta = 0.20$ ,  $\delta = 0.167$  and  $U_A = 2.87$  and the lower dotted one to  $I_\theta = 0.21$ ,  $\delta = 0.079$  and  $U_A = 3.70$ , all at a lowered effective charge  $\bar{Z}$ .

**Fig. 4:** Experimental data of the second virial coefficient  $B_2$  of lysozyme as a function of the ionic strength  $I$  at a pH of about 7.5. The second virial coefficient is scaled by the hard sphere value  $B_2^{HS}$ . Black stars: Rosenbaum et al. [20], pH 7.4, 25°C; black triangles: Velev et al. [21], pH 7.5, 25°C; black squares: Rosenbaum et al. [14], pH 7.8, 25°C.

**Fig. 5:** Fits of Eq. (28) to experimental data of Fig. 3. Full line ( $Z_{eff}$  and  $\delta \exp U_A = 4.2$ ); Dotted line ( $\bar{Z}$  and  $\delta \exp U_A = 3.7$ ).

**Fig. 6:** Comparison between the experimental data at pH 7.5 and full theory Eq. (5). Parameters as in the lower dotted curve in Fig. 3 ( $\delta = 0.079$  and  $U_A = 3.70$ ).

**Fig. 7:** Ionic-strength dependence of AHS parameter  $\tau$  at pH 4.5 and pH 7.5. The dotted line denotes the limiting value of  $\tau$  as  $I \rightarrow \infty$ .

**Fig. 8:** Inverse osmotic compressibility as a function of the volume fraction  $\eta$  at various

ionic strengths. Experimental data: black squares:  $I = 0.18$  M; black triangles:  $I = 0.23$  M; black stars:  $I = 0.28$  M; black diamonds:  $I = 0.33$  M; open squares:  $I = 0.48$  M. All data from Rosenbaum et al. [14], except for those at  $I = 0.23$  M (black triangles) (Piazza et al. [13]). Curves computed from Eq. (54) with  $\delta = 0.079$ ,  $U_A = 3.70$  and the lowered effective charge  $\bar{Z}$ ;  $\tau$  has been determined from Eq. (53). From top to bottom:  $I = 0.18$  M,  $I = 0.23$  M,  $I = 0.28$  M,  $I = 0.33$  M and  $I = 0.48$  M.

**Fig. 9:** Dependence of  $\ln \xi$  on  $\mu$  at pH 4.5 and pH 7.5. In both cases  $d \ln \xi / d\mu < 0$  and  $d^2 \ln \xi / d\mu^2 \gtrsim 0$  if  $1 \leq \mu \leq 8$ .

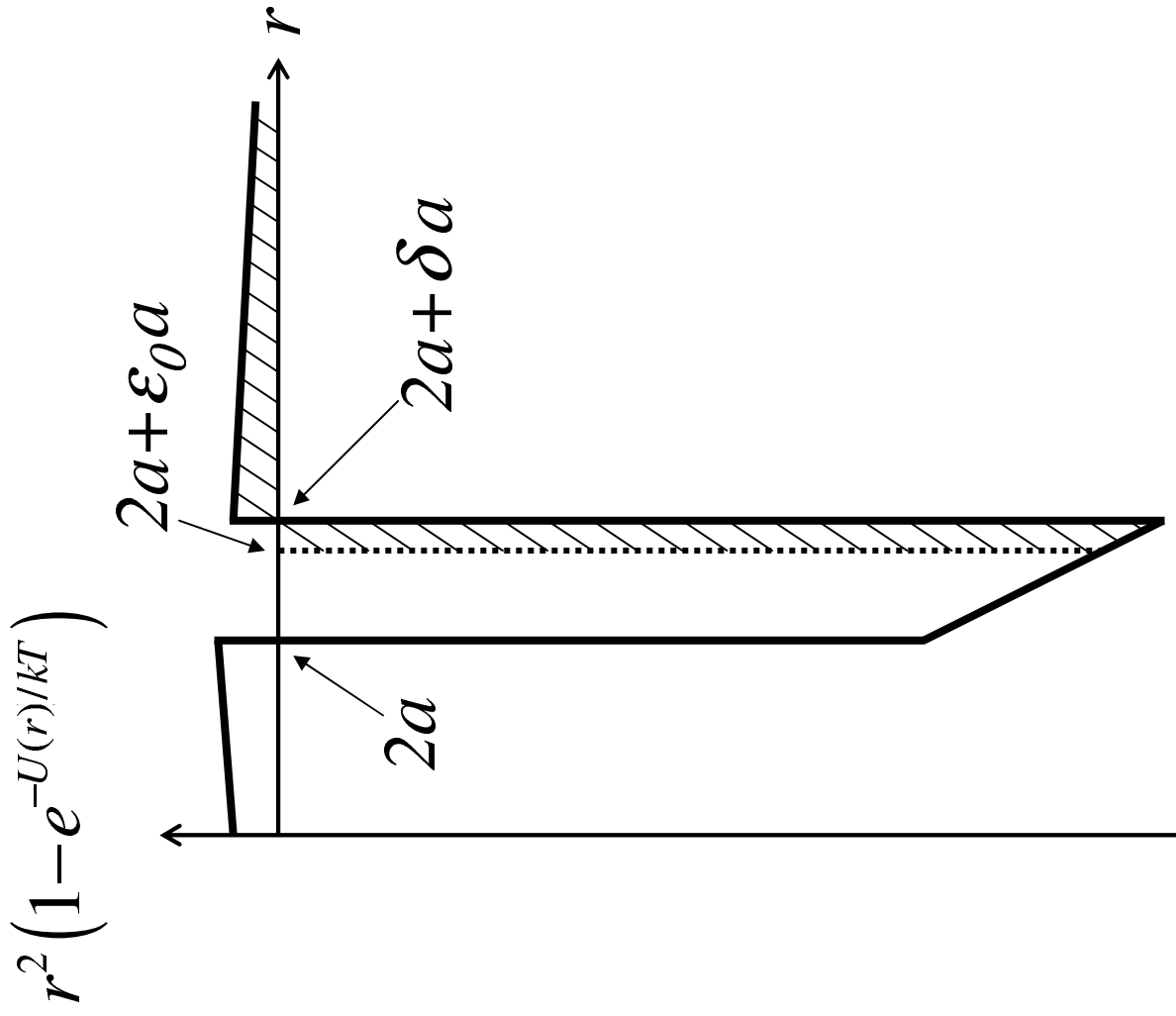


Fig. 1 - Prinsen & Odijk



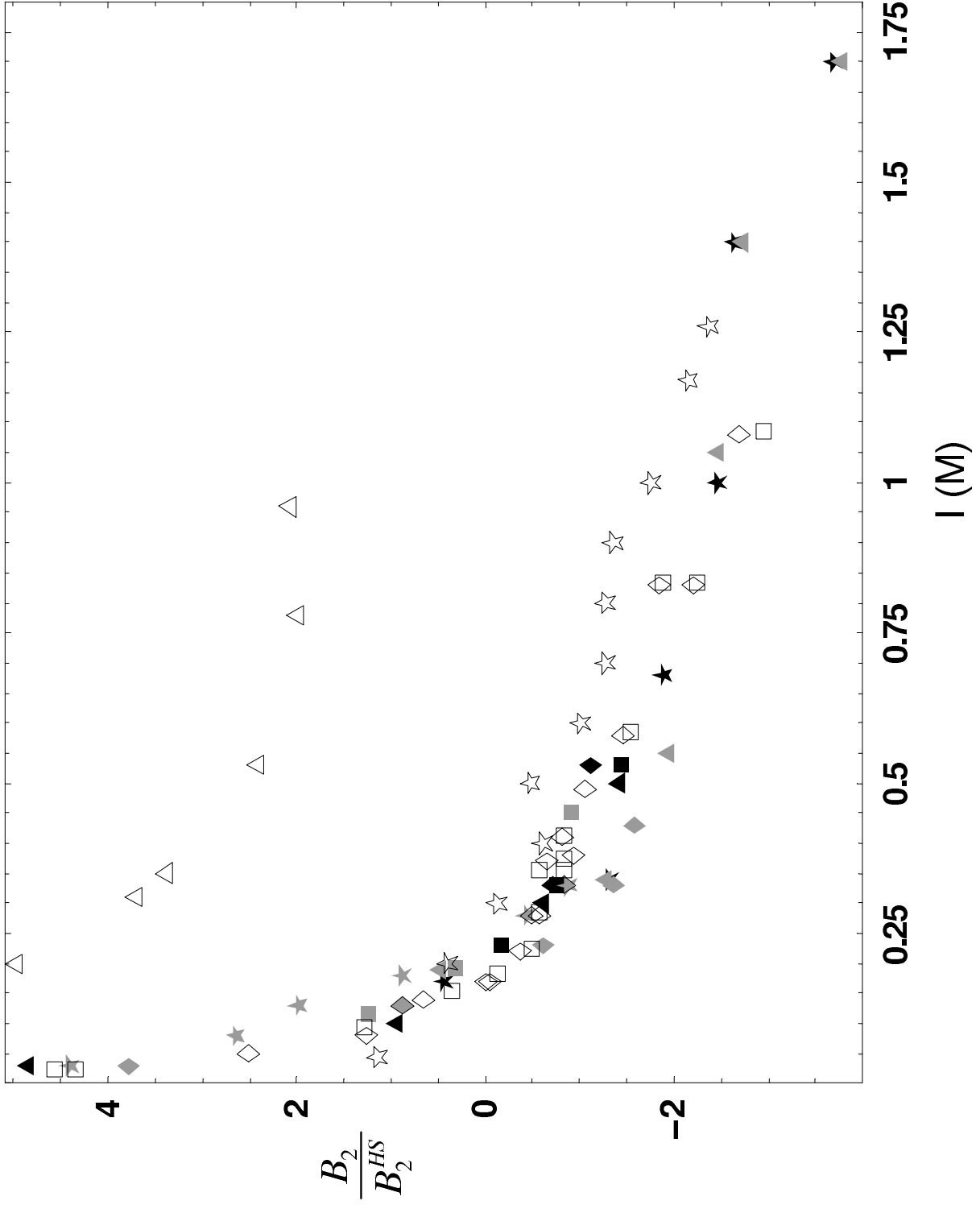


Fig. 2 - Prinsen & Odijk

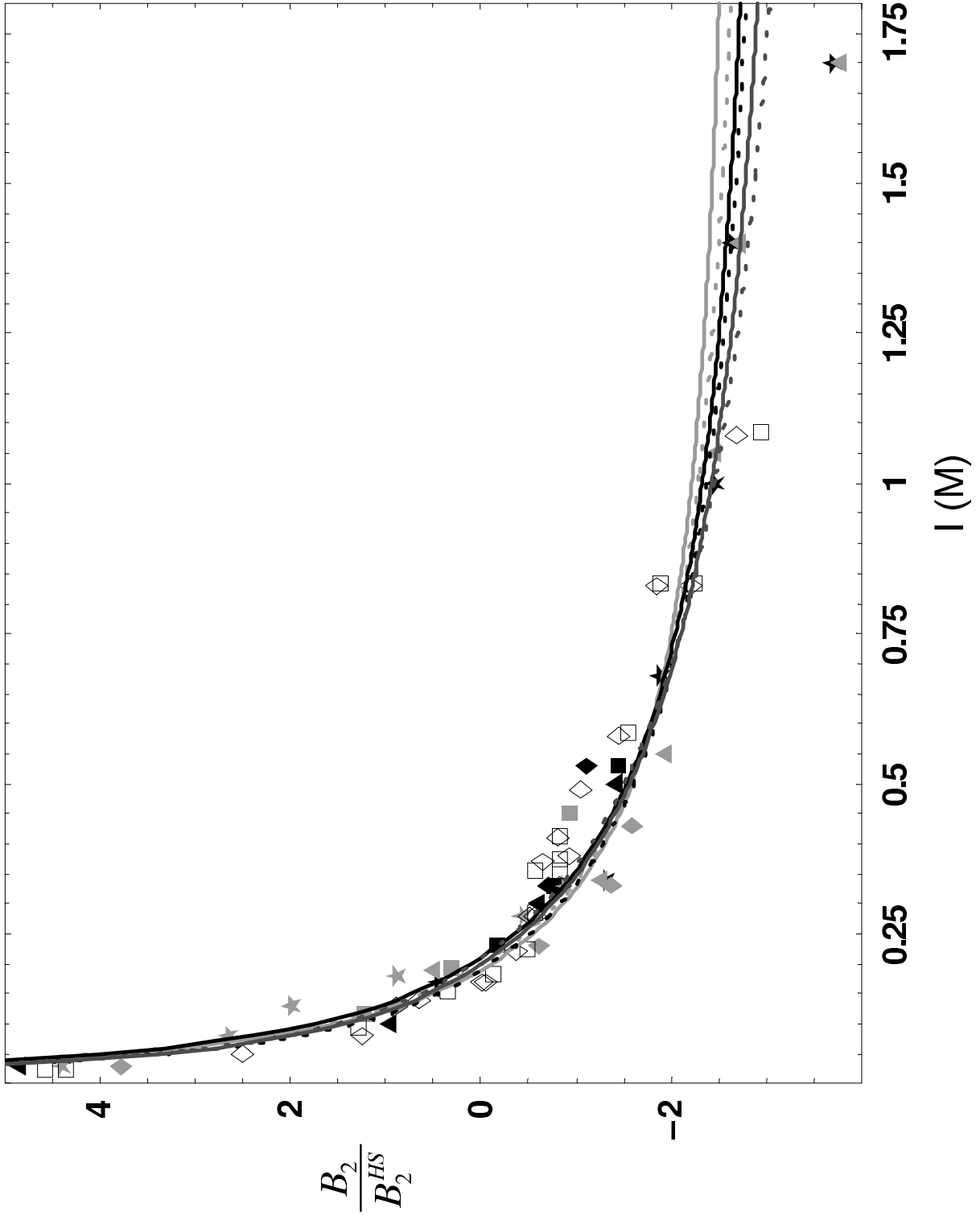


Fig. 3 - Prinsen & Odijk

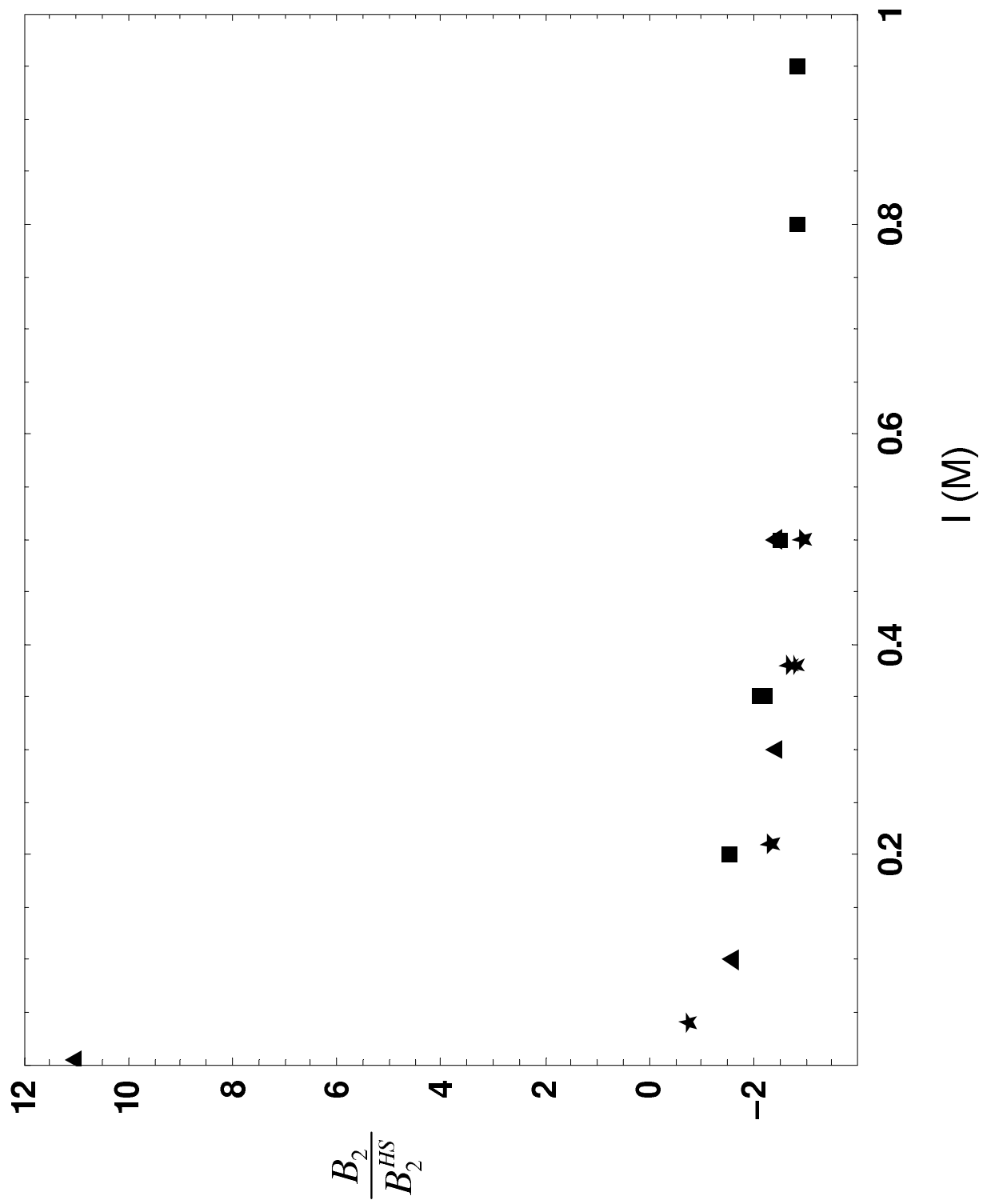


Fig. 4 - Prinsen & Odijk

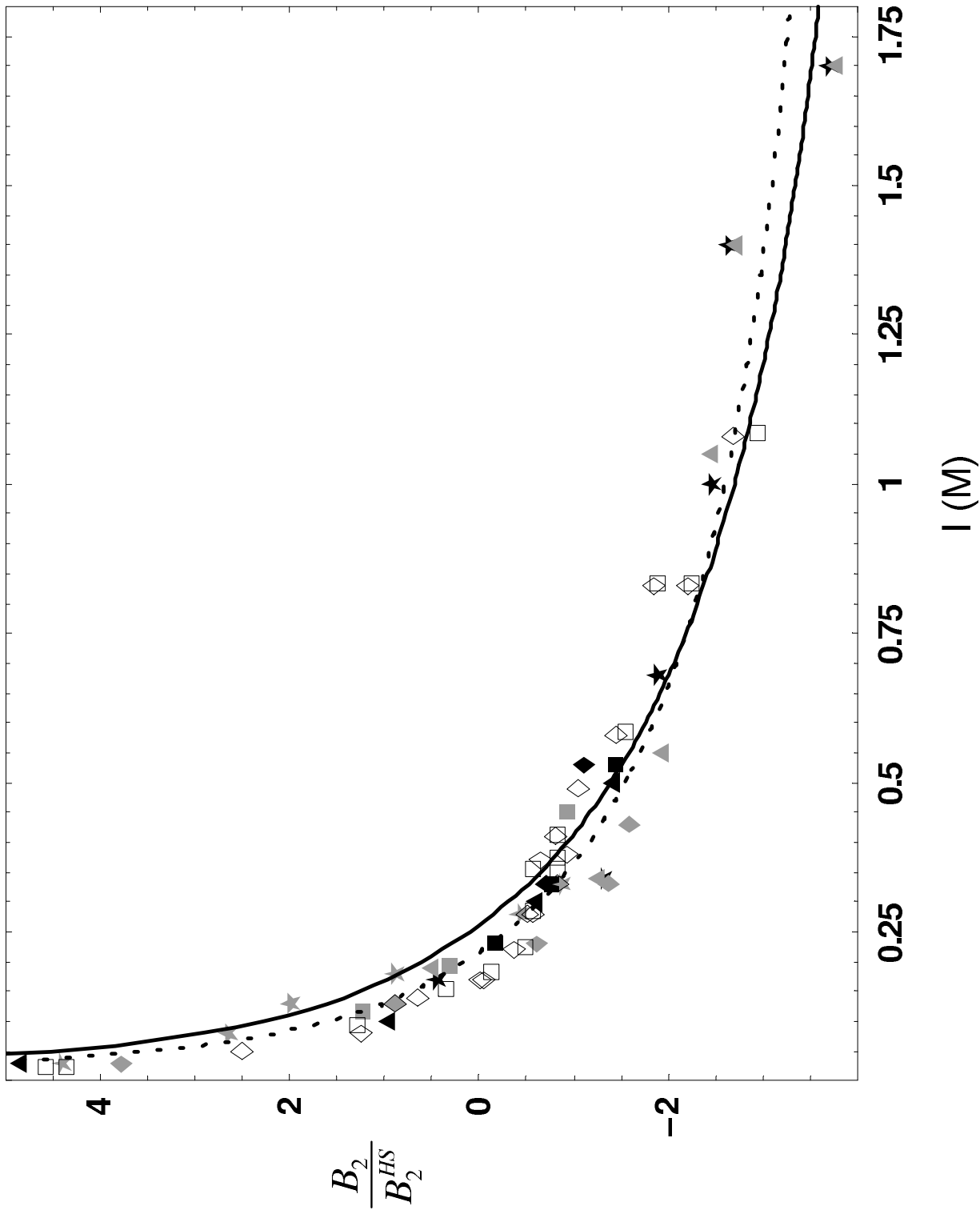


Fig. 5 - Prinsen & Odijk

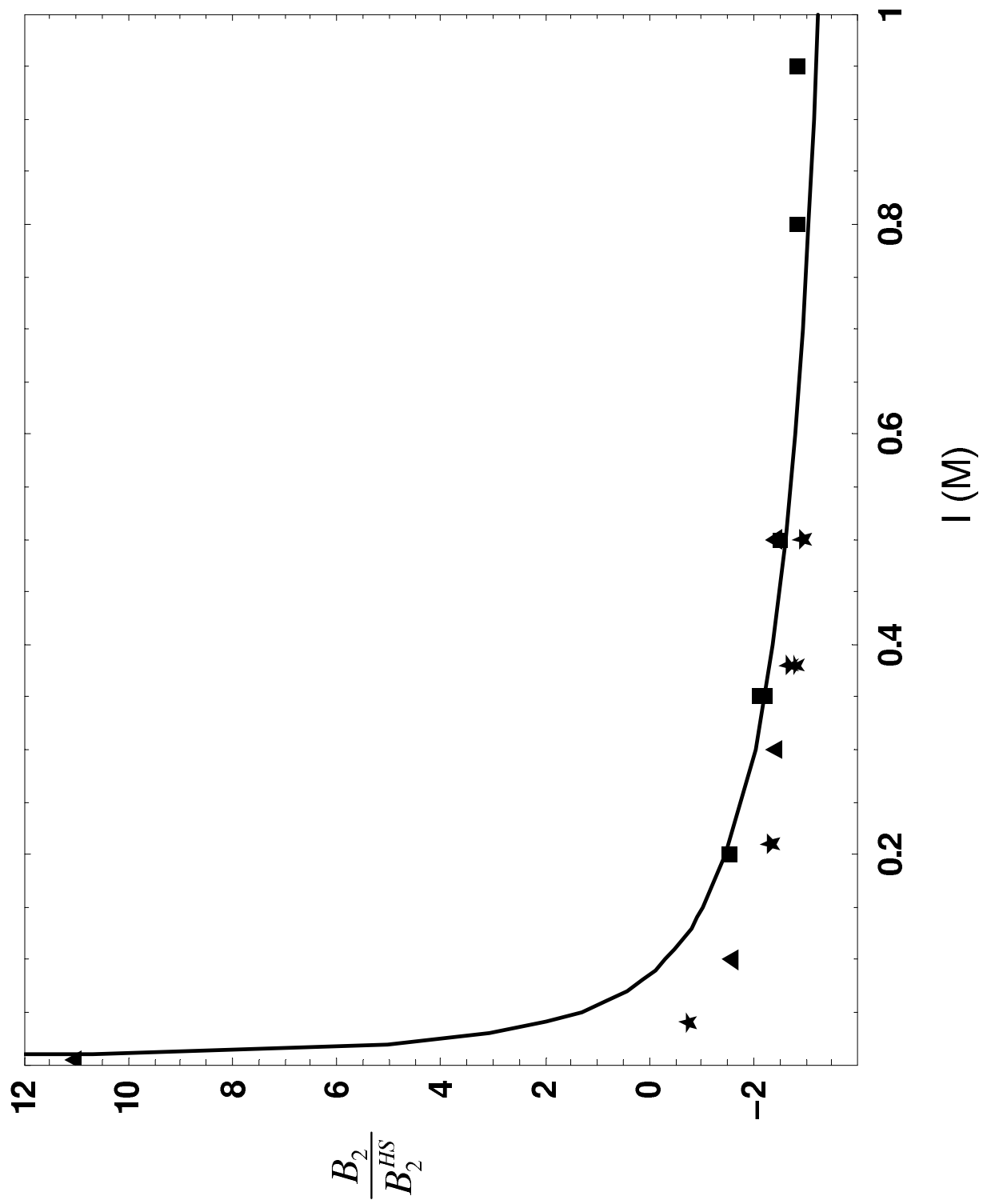


Fig. 6 - Prinsen & Odijk

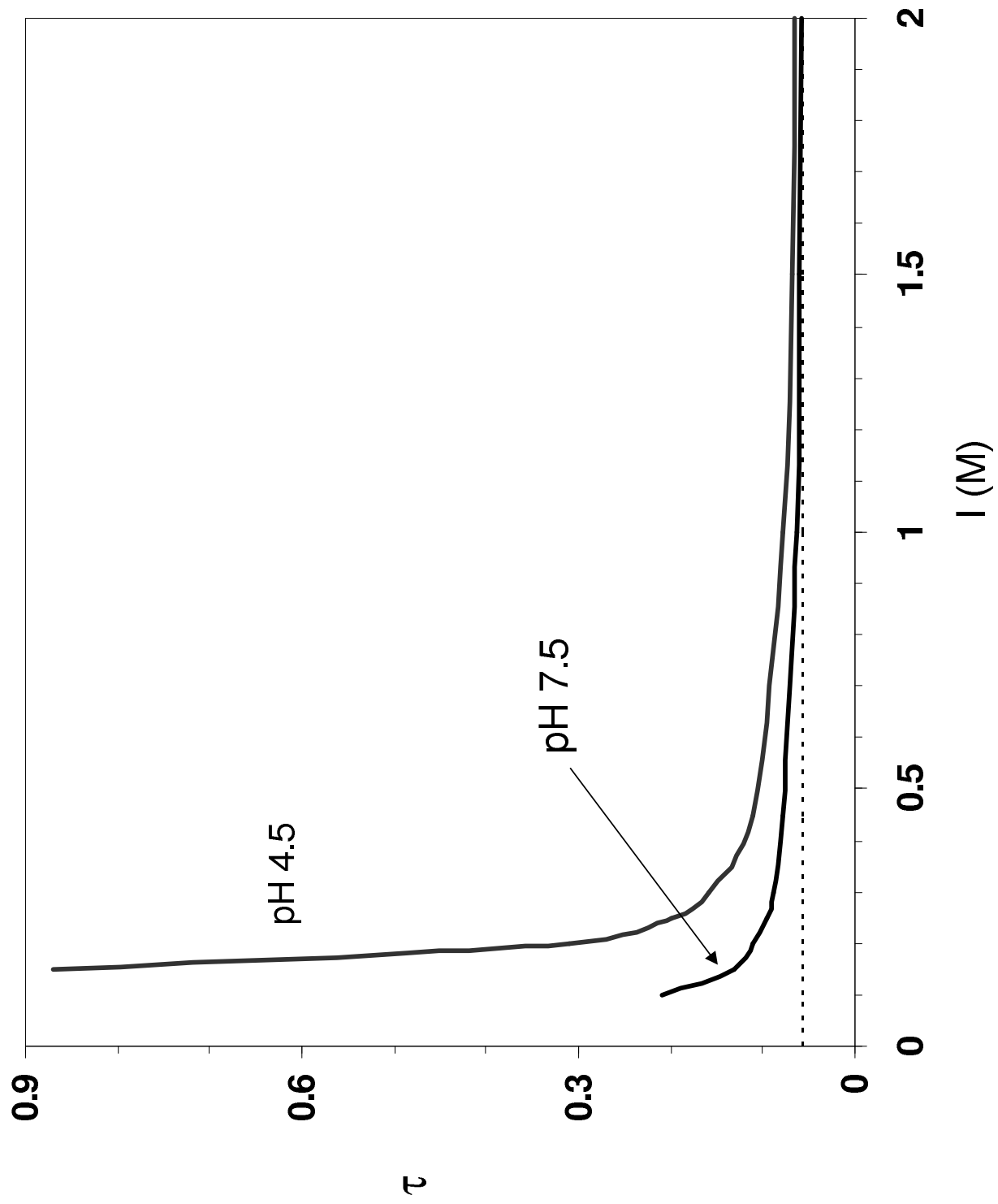


Fig. 7 - Prinsen & Odijk

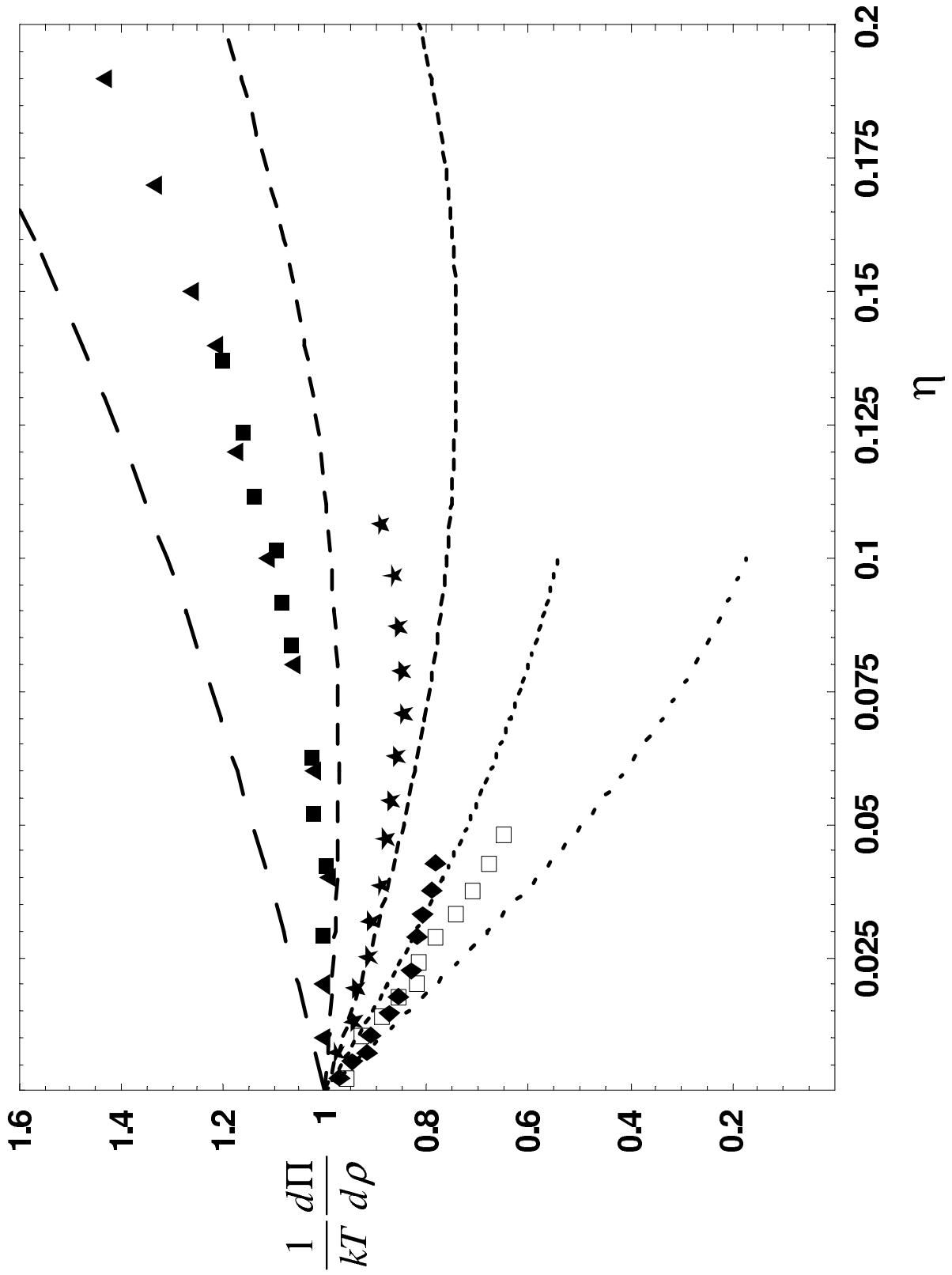


Fig. 8 - Prinsen & Odijk

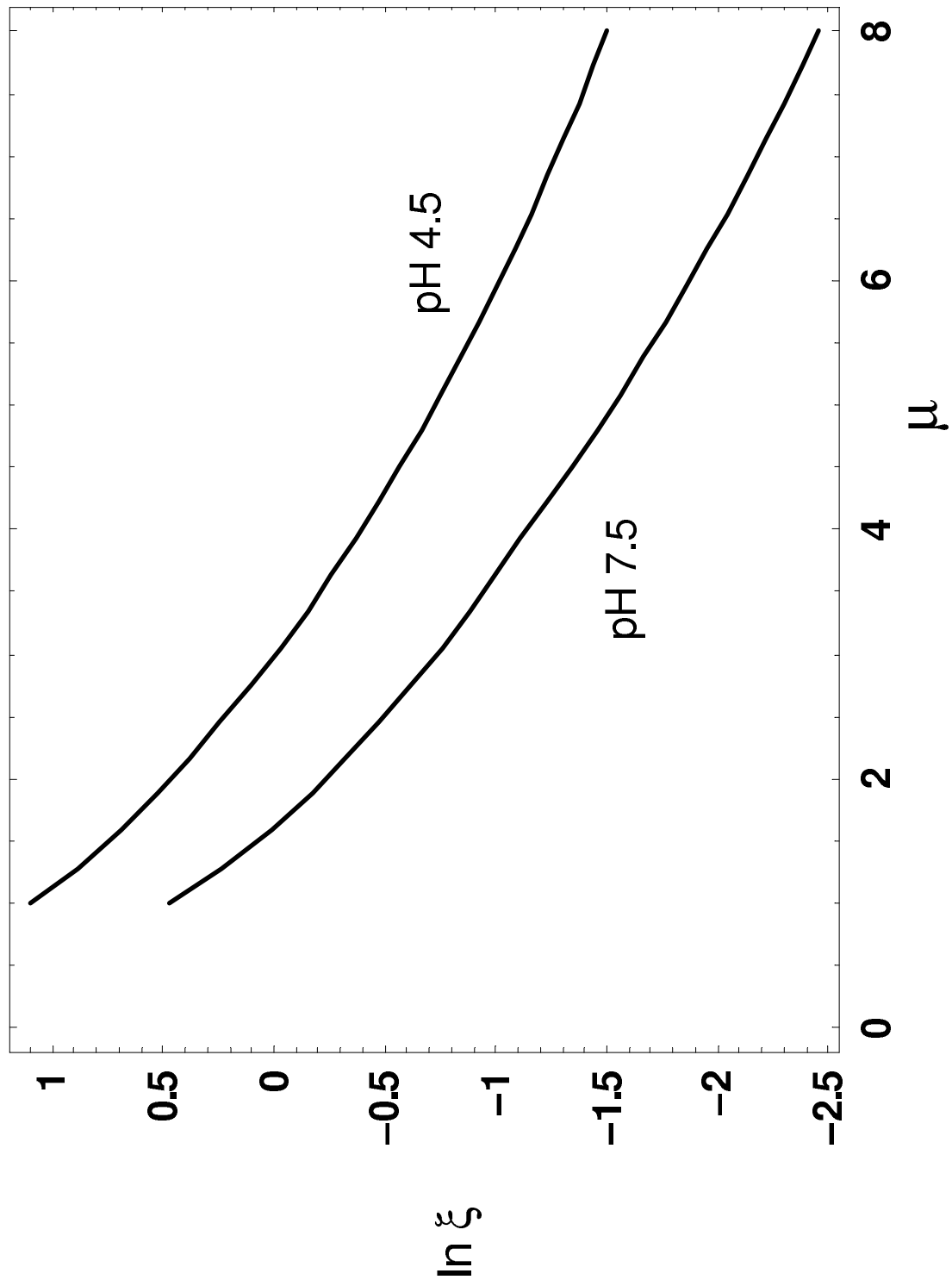


Fig. 9 - Prinsen & Odijk